UNIVERSIDADE D
COIMBRA

Joana Sofia da Silva Domingues

ASTROCYTIC CONNEXIN 43 HEMICHANNELS ACTIVITY UNDER ALZHEIMER'S DISEASE-LIKE CONDITIONS: REGULATION BY ADENOSINE A_{2A} RECEPTORS

Dissertação no âmbito do Mestrado em Engenharia Biomédica com Especialização em Neurociências, orientada pela Professora Doutora Paula Maria Garcia Agostinho, e apresentada ao Departamento de Física da Faculdade de Ciências e Tecnologia da Universidade de Coimbra.

Janeiro de 2023

UNIVERSIDADE D
COIMBRA

Joana Sofia da Silva Domingues

Astrocytic connexin 43 hemichannels activity under Alzheimer's disease-like conditions: Regulation by adenosine A_{2A} receptors

Dissertação apresentada ao Departamento de Física da Faculdade de Ciências e Tecnologia da Universidade de Coimbra, para cumprimento dos requisitos necessários à obtenção do grau de Mestre em Engenharia Biomédica na Área de Especialização de Neurociências, realizada sob orientação científica da Professora Doutora Paula Maria Garcia Agostinho.

Coimbra
2023

The present work was performed at the Center for Neuroscience and Cell Biology (CNC) of the University of Coimbra, in the research group "Purines at CNC – Neuromodulation Group", under scientific guidance of Professor Doctor Paula Agostinho.

The work was funded by *Fundação "la Caixa"* (HP17/00523), *Centro 2020* (CENTRO-01–0145-FEDER-000008:BrainHealth 2020 and CENTRO-01–0246-FEDER-000010) and *Fundação para a Ciência e a Tecnologia* (FCT, PTDC/MED-NEU/31274/2017 and UIDB/04539/2020).

Aos meus pais e irmão,
pelo amor incondicional.
Aos meus avós,
pelos valores transmitidos.
Aos meus queridos amigos Inês e Ângelo,
pela empatia constante.
À restante família e amigos.

À Professora Doutora Paula Agostinho, a minha Orientadora.
Às alunas de doutoramento Daniela Madeira e Cátia Lopes, com quem trabalhei mais proximamente.
Às colegas Ingride Gaspar, Joana Santos e Joana Silva, que foram um apoio importante neste último ano.
Ao Professor Doutor Rodrigo Cunha, o líder do grupo de investigação que integrei.
Aos restantes membros do grupo.

Muito obrigada!

I hope the readers of this thesis may find the following lines as funny as I do...:

> *I am passionate about Music. Close to completing my Final Master's Project, I listened to a conceptual album ("Ziltoid the Omniscient", by Devin Townsend), about an extraterrestrial who comes to Earth to have the human's "ultimate cup of coffee". When a coffee is delivered to him, he finds it "fetid" and decides to attack Earth. I immediately thought of mentioning this album here, since my research group is inspired by the effects of caffeine on the nervous system; indeed, the only known molecular targets of caffeine are adenosine receptors.*

RESUMO

Acredita-se que a doença de Alzheimer (DA), considerada como a forma mais comum de demência no idoso, seja impulsionada pela deposição de péptidos β-amiloide (Aβ) no cérebro. Perto dos depósitos de Aβ, os astrócitos parecem exibir uma remodelação morfofuncional, contribuindo para o fenótipo da DA. Evidências acumuladas sugerem uma sobrerregulação da conexina 43 (Cx43) astrocítica, a principal proteína que forma hemicanais nos astrócitos, assim como um aumento da atividade dos hemicanais astrocíticos compostos por Cx43 (Cx43 HC), em condições de DA. Nos astrócitos, os HC medeiam a libertação de gliotransmissores, nomeadamente ATP, a molécula energética que é considerada como um sinal de perigo quando fora das células. A cafeína é cada vez mais reconhecida por ter um efeito protetor contra a DA e especula-se que este efeito seja devido ao bloqueio dos recetores de adenosina A_{2A} ($A_{2A}R$) mediado pela cafeína. Uma vez que os Cx43 HC astrocíticos podem libertar ATP e os $A_{2A}R$ podem ser ativados por adenosina derivada do ATP, nós levantámos a hipótese de que os $A_{2A}R$ poderiam regular a atividade dos Cx43 HC astrocíticos. Recentemente, usando culturas primárias de astrócitos expostas a péptidos $A\beta_{1-42}$ sintéticos, nós identificámos um círculo vicioso através do qual os $A_{2A}R$ regulam a atividade dos Cx43 HC, levando ao aumento da libertação de ATP, que é convertido em adenosina pela ecto-5'-nucleotidase (CD73), sobreativando os $A_{2A}R$.

No presente estudo, nós investigámos a suposta regulação da atividade dos Cx43 HC astrocíticos mediada pelos $A_{2A}R$ em fatias do hipocampo, que representam um sistema biológico mais integrado, onde além de astrócitos existem outras células cerebrais que estabelecem interações físicas e funcionais umas com as outras. Condições de DA foram mimetizadas através da exposição *ex vivo* de fatias hipocampais de murganhos a $A\beta_{1-42}$ e evoluíram para modelos de DA em murganhos, nomeadamente murganhos injetados intracerebroventricularmente (icv) com $A\beta_{1-42}$ recapitulando a forma esporádica da DA, e murganhos transgénicos APP/PS1 modulando a forma familiar da DA. Além disso, combinaram-se ferramentas farmacológicas e genéticas para explorar o controlo agudo ou a longo prazo da atividade dos Cx43 HC astrocíticos pelos $A_{2A}R$. A permeabilização da membrana mediada pelos HC foi avaliada através da captação de brometo de etídio (EtBr), um marcador fluorescente que passa através dos HC e se acumula no núcleo das células, e para garantir que estamos a quantificar a atividade dos HC nos astrócitos nós realizámos

imunohistoquímica para marcar os astrócitos para a proteína acídica fibrilar glial (GFAP), um marcador astrocítico amplamente usado. Notavelmente, este trabalho também contribuiu para estabelecer uma nova metodologia no nosso grupo, consistindo de um protocolo de processamento e análise de imagem tridimensional para quantificação da intensidade de fluorescência do EtBr por volume do núcleo dos astrócitos, providenciando assim informação mais precisa acerca da atividade dos HC nos astrócitos.

Observou-se que a exposição *ex vivo* de fatias hipocampais de murganhos C57BL/6 a $A\beta_{1-42}$ aumentou significativamente a captação de EtBr, o que indica um aumento da atividade dos HC nos astrócitos (células imuno-positivas para o GFAP), sendo este efeito prevenido pelo bloqueio dos $A_{2A}R$. Em contraste, nem o bloqueio dos $A_{2A}R$ diretamente, nem da fonte de adenosina que ativa os $A_{2A}R$, isto é, da CD73, reverteu o aumento da atividade dos HC astrocíticos no hipocampo de murganhos injetados icv com $A\beta_{1-42}$ e de murganhos APP/PS1. Observou-se também que o silenciamento dos $A_{2A}R$ completo ou especificamente nos astrócitos, mas não especificamente nos neurónios, preveniu o aumento da atividade dos HC induzido pelo $A\beta_{1-42}$ em astrócitos hipocampais, demonstrando que os $A_{2A}R$ astrocíticos têm um papel principal na regulação da atividade dos HC astrocíticos sob desafio com $A\beta_{1-42}$. Além disso, o bloqueio dos Cx43 HC reduziu o aumento da atividade dos HC astrocíticos no hipocampo de murganhos APP/PS1 para o nível de murganhos WT, revelando que os Cx43 HC astrocíticos estão preferencialmente ativados nestes animais.

Em conjunto, os nossos resultados reforçam o suposto papel dos $A_{2A}R$ astrocíticos na regulação da atividade dos Cx43 HC astrocíticos, previamente observado em astrócitos cultivados e aqui em astrócitos hipocampais. A demonstração de que a disrupção da atividade dos $A_{2A}R$ astrocíticos previne a sobreativação dos Cx43 HC astrocíticos no hipocampo de murganhos sugere que os $A_{2A}R$ astrocíticos são um alvo farmacológico alternativo valioso em fases precoces da DA.

Palavras-chave: doença de Alzheimer, astrócitos, hemicanais compostos por conexina 43, recetores de adenosina A_{2A}

ABSTRACT

Alzheimer's disease (AD), considered as the most common form of dementia in the elderly, is believed to be driven by the deposition of amyloid-β peptides (Aβ) in the brain. Near Aβ deposits, astrocytes appear to exhibit a morphofunctional remodeling, contributing to AD phenotype. Accumulating evidences suggest an upregulation of astrocytic connexin 43 (Cx43), the major hemichannel-forming protein in astrocytes, as well as an enhancement of the activity of astrocytic Cx43 hemichannels (Cx43 HC), under AD-like conditions. In astrocytes, HC mediate the release of gliotransmitters, namely ATP, the energetic molecule that is considered as a danger signal when outside the cells. Caffeine is increasingly recognized to have a protective effect against AD and this effect is speculated to be due to caffeine-mediated blockade of adenosine A_{2A} receptors ($A_{2A}R$). Since astrocytic Cx43 HC can release ATP and the $A_{2A}R$ can be activated by adenosine derived from ATP, we hypothesized that $A_{2A}R$ might regulate astrocytic Cx43 HC activity. Recently, using primary astrocyte cultures exposed to synthetic $A\beta_{1-42}$ peptides, we identified a vicious circle whereby $A_{2A}R$ regulate Cx43 HC activity, leading to increased ATP release, which is converted into adenosine by ecto-5'-nucleotidase (CD73), overactivating $A_{2A}R$.

In the present study, we investigated the putative $A_{2A}R$-mediated regulation of astrocytic Cx43 HC activity in hippocampal slices, which represent a more integrated biological system, where besides astrocytes there are other brain cells that establish physical and functional interactions with each other. AD conditions were mimicked through *ex vivo* exposure of mouse hippocampal slices to $A\beta_{1-42}$ and evolved to AD mouse models, namely mice injected intracerebroventricularly (icv) with $A\beta_{1-42}$ recapitulating sporadic AD, and APP/PS1 transgenic mice modeling familial AD. Moreover, pharmacological and genetic tools were combined to explore the acute or long-term control of astrocytic Cx43 HC activity by $A_{2A}R$. HC-mediated membrane permeabilization was evaluated through the uptake of ethidium bromide (EtBr), a fluorescent tracer that passes through HC and accumulates in cell nuclei, and to ensure that we are quantifying HC activity in astrocytes we performed immunohistochemistry to label astrocytes for glial fibrillary acidic protein (GFAP), a widely used astrocytic marker. Noteworthy, this work also contributed to establish a novel methodology in our group, consisting of a three-dimensional image processing and analysis protocol for quantification of EtBr fluorescence intensity per

astrocyte nucleus volume, thus providing more accurate information about HC activity in astrocytes.

It was observed that *ex vivo* exposure of hippocampal slices from C57BL/6 mice to $A\beta_{1-42}$ significantly increased EtBr uptake, which indicates an enhancement of HC activity in astrocytes (GFAP immuno-positive cells), being this effect prevented by $A_{2A}R$ blockade. In contrast, neither blocking $A_{2A}R$ directly nor the source of adenosine that activates $A_{2A}R$, that is, CD73, reversed the increased astrocytic HC activity in the hippocampus of icv-$A\beta_{1-42}$-injected mice and APP/PS1 mice. It was also observed that full or astrocyte-specific, but not neuron-specific, $A_{2A}R$ silencing prevented $A\beta_{1-42}$-induced increase in HC activity in hippocampal astrocytes, demonstrating that astrocytic $A_{2A}R$ have a major role in the regulation of astrocytic HC activity upon $A\beta_{1-42}$ challenge. Furthermore, Cx43 HC blockade reduced the increased astrocytic HC activity in the hippocampus of APP/PS1 mice to the level of WT mice, revealing that astrocytic Cx43 HC are preferentially activated in these animals.

Overall, our results strengthen the putative role of astrocytic $A_{2A}R$ in the regulation of astrocytic Cx43 HC activity, previously observed in cultured astrocytes and here in hippocampal astrocytes. The demonstration that the disruption of astrocytic $A_{2A}R$ activity prevents astrocytic Cx43 HC overactivation in the mouse hippocampus suggests that astrocytic $A_{2A}R$ are an alternative valuable pharmacological target at early stages of AD.

Keywords: Alzheimer's disease, astrocytes, connexin 43 hemichannels, adenosine A_{2A} receptors

TABLE OF CONTENTS

LIST OF FIGURES

LIST OF ABBREVIATURES

$[Ca^{2+}]_i$ – Intracellular Ca^{2+} concentration
A_1R – Adenosine A_1 receptors
$A_{2A}R$ – Adenosine A_{2A} receptors
AAV5 – Adeno-associated virus serotype 5
ACSF – Artificial cerebrospinal fluid
AD – Alzheimer's disease
AMP – Adenosine monophosphate
AP – Anteroposterior
APOE – Apolipoprotein E
APP – Amyloid precursor protein
ATP – Adenosine triphosphate
Aβ – Amyloid-β peptides
BACE – β-secretase
C57BL/6 – C57 black 6
CA1 – *Cornu ammonis* 1
cAMP – Cyclic AMP
CBX – Carbenoxolone disodium salt
CD73 – Ecto-5′-nucleotidase
CMLE – Classic maximum likelihood estimation
CNS – Central nervous system
Cre – Cre recombinase
CREB – cAMP response element-binding protein
CTR – Control
Cx – Connexin
DNA – Deoxyribonucleic acid
DV – Dorsoventral
EAAT1/2 – Excitatory amino acid transporter 1/2
ENT – Equilibrative nucleoside transporters
EtBr – Ethidium bromide
Fb – Forebrain
FRAP – Fluorescence recovery after photobleaching
Gb – Global
GFAP – Glial fibrillary acidic protein
GFP – Green fluorescent protein
GJ – Gap junctions
GJA1 – Cx43 encoding gene
GJC – Gap junction channels
GLAST – Glutamate-aspartate transporter
GLT1 – Glutamate transporter 1
GSK3 – Glycogen synthase kinase 3
HC – Hemichannels
HS – Horse serum
icv – Intracerebroventricular
IP_3 – Inositol triphosphate

KO – Knockout
KW 6002 – Istradefylline
La^{3+} – Lanthanum trichloride ($LaCl_3$)
LSM – Laser scanning microscope
LTP – Long-term potentiation
MAPK – Mitogen-activated protein kinase
MK 801 – Dizocilpine
ML – Mediolateral
NFT – Neurofibrillary tangles
NFκB – Nuclear factor κ B
NMDAR – N-methyl-D-aspartate receptors
P_1R – Purinergic P_1 receptors
P_2R – Purinergic P_2 receptors
P_2XR – Ionotropic P_2R
P_2YR – Metabotropic P_2R
Panx – Pannexin
PBS – Phosphate buffered saline
PFA – Paraformaldehyde
PKA – Protein kinase A
PS1/2 – Presenilin 1/2
PSF – Point spread function
RNA – Ribonucleic acid
RT – Room temperature
SEM – Standard error of the mean
SR101 – Sulforhodamine 101
VEH – Vehicle
WT – Wildtype

CHAPTER I

Introduction

1. Alzheimer's disease: Focus on amyloid-β peptides

Alzheimer's disease (AD) is an age-related neurodegenerative disorder that causes deficits of memory and other cognitive functions, alterations of behavior and personality, among others, and those symptoms usually manifest several decades after the disease onset (reviewed in Guo et al., 2020). Although AD is considered the most common form of dementia in the elderly, there is still no effective treatment for this disorder. Indeed, most anti-AD drugs currently on the market, acetylcholinesterase inhibitors and N-methyl-D-aspartate receptor (NMDAR) antagonists, besides being symptomatic and not disease-modifying, are associated with few benefits and many adverse side-effects (reviewed in Cummings et al., 2022). Current research for disease-modifying therapies has focused on two proteins that aggregate and become pathogenic in AD, the amyloid-β (Aβ) and tau proteins (Guo et al., 2020). It is worth mentioning that aducanumab, a monoclonal antibody directed against Aβ oligomers, was recently approved for treatment of AD by Food and Drug Administration (FDA) (Cummings et al., 2022).

Aβ is produced through the proteolytic cleavage of amyloid precursor protein (APP), a transmembrane protein whose physiological function remains unclear (reviewed in Guo et al., 2020). APP can be processed through two distinct mechanisms. Accordingly, in the non-amyloidogenic pathway, α- and γ-secretases cleave APP sequentially, which does not result in the generation of Aβ species. On the other hand, in the amyloidogenic pathway, APP is first cleaved by β-secretase (also known as BACE) and then by γ-secretase, followed by the release of Aβ peptides, mainly $A\beta_{1-40}$ and $A\beta_{1-42}$, being the 40-amino acid form the most abundant and the 42-amino acid form the most prone to aggregation. In the extracellular medium, monomeric Aβ aggregates to form oligomers, protofibrils, fibrils and, ultimately, plaques (Guo et al., 2020). In turn, tau, which is a microtubule-binding protein important for axonal microtubule stability, becomes hyperphosphorylated in AD, forming intracellular aggregates called neurofibrillary tangles (NFT) (Guo et al., 2020).

Elevation of brain Aβ levels may occur due to either: 1) mutations in the genes encoding for APP, or presenilin 1 (PS1) or 2 (PS2), the catalytic subunit of γ-secretase, increasing Aβ production (in the case of familial AD), or 2) deficient Aβ clearance, which can be attributed, but not restricted, to apolipoprotein E4 (APOE4) inheritance, since APOE4 is less effective in clearing Aβ compared to other APOE forms (in the case of sporadic AD) (reviewed in Hardy and Selkoe, 2002). According to the prevailing amyloid cascade hypothesis, accumulation and oligomerization of Aβ is the initial event of AD pathogenesis. Accumulating evidences indicate that soluble Aβ oligomers, rather than monomers or insoluble fibrillar forms, are the most neurotoxic Aβ species, injuring synapses and neurons. Consequently, altered kinase/phosphatase activity promotes tau hyperphosphorylation and aggregation, leading to widespread synaptic dysfunction and neuronal damage, cognitive impairment and, finally, dementia (Hardy and Selkoe, 2002).

At the twenty-five years of the amyloid cascade hypothesis, Selkoe and Hardy reviewed the findings that undergird, as well as the ones that undermine, this hypothesis, the latter including: 1) weak correlation between Aβ plaques and cognitive impairment compared to NFT, 2) tau pathology may precede Aβ deposition, 3) Aβ deposits may be detected in cognitively healthy subjects, and 4) numerous clinical trials of anti-Aβ agents that have not met clinical efficacy (reviewed in Selkoe and Hardy, 2016). The authors' respective counterarguments are that: 1) Aβ deposition is a very early event that can lead to many downstream effects, including tau pathology, which, in turn, are more proximate to and causative of cognitive impairment, 2) studies do not have searched systematically for diffuse plaques or oligomers of Aβ, 3) many Aβ deposits are diffuse plaques (not rich in abnormal neurites and glia), and 4) most failed trials enrolled patients with mild to moderate AD and/or without evidence of Aβ deposition, whereas trials in patients at earlier stages of biomarker-confirmed AD are producing better results (Selkoe and Hardy, 2016).

Many consequences of AD are attributed to neuronal damage and death, but glial cells are increasingly considered as important players in this pathology. Indeed, a pathological hallmark of AD, in addition to Aβ plaques and NFT, is gliosis associated with Aβ plaques, where activated microglia and astrocytes are recruited, secreting proinflammatory factors and phagocytizing Aβ (reviewed in Frost et al., 2017). Although neurons are considered the main source of Aβ, reactive astrocytes display an upregulation of the three molecular agents required for Aβ production: APP (*e.g.*, Haass et al., 1991), β-secretase (*e.g.*, Hartlage-Rübsamen et al., 2003) and γ-secretase (*e.g.*, Diehlmann et al.,

1999). Since astrocytes are an abundant cell type in the brain, a smaller amount of Aβ secreted by individual astrocytes might be substantial. In response to increased Aβ levels, the release of proinflammatory factors by microglia and astrocytes also increases, leading to excessive neuroinflammation (Frost et al., 2017).

2. Astrocytes: Network organization and functions

Astrocytes tile the entire central nervous system (CNS) without overlapping each other, and these glial cells are provided with several processes that establish physical and functional interactions with neuronal, other glial and blood vessel cells (reviewed in Sofroniew and Vinters, 2010). Based on astrocyte morphology and location, the two major types of astrocytes considered are the protoplasmic (highly branched processes) and fibrous (long processes), being the protoplasmic prominently found in gray matter, whereas the fibrous are most abundant in white matter of both brain and spinal cord (Sofroniew and Vinters, 2010).

Although, until a few years ago, astrocytes were merely considered as support cells, they are currently recognized as active brain elements, controlling numerous brain homeostatic functions. Astrocytes have a key role in modulating neuronal synaptic transmission and plasticity, the latter being considered as the neurophysiological basis of memory (reviewed in Oliveira et al., 2015). According to the concept of tripartite synapse (Araque et al., 1999), fine astrocytic processes that enwrap pre- and post- synaptic terminals, named perisynaptic processes, are able to respond to neurotransmitters released during neuronal activity and also to release neuroactive substances, called gliotransmitters, that influence neuronal activity (reviewed in Halassa and Haydon, 2010 and Nedergaard and Verkhratsky, 2012). It is worth mentioning that astrocytes do not surround all synapses, but in the hippocampus 60-90% of the synapses are covered by astrocytic processes, whose structural modification can greatly impact synaptic function (Ventura and Harris, 1999).

Besides the local control of synaptic function by astrocytic processes that enwrap neuronal synapses, astrocytes are able to form networks where neuronal circuits are embedded, the so-called astrocytic syncytia, being responsible for a slow integration of information from thousands of synapses to adjust the overall functioning of the neuronal circuitry (reviewed in Halassa and Haydon, 2010 and Nedergaard and Verkhratsky, 2012). The network organization of astrocytes allows them to communicate through specialized

intercellular channels, referred to as gap junctions (GJ), which are formed by connexin (Cx) proteins, mainly Cx30 and Cx43 (reviewed in Giaume et al., 2010). Briefly, connexins are transmembrane proteins that oligomerize into hexamers referred to as connexons. Two juxtaposed connexons from different cells form gap junction channels (GJC). Junctional plaques, consisting of series of a few tens to thousands of GJC, allow the diffusion of small molecules to distant cells, including ions (Ca^{2+}, Na^{+}, K^{+}), amino acids (glutamate, glutathione), second messengers (ATP, cAMP, IP_3) and metabolites (glucose, lactate). Connexins also function as unitary channels called hemichannels (HC), which mediate the local release of gliotransmitters (ATP, glutamate). HC may also be comprised of pannexin (Panx) proteins, mainly Panx1, but these proteins do not form GJC. Noteworthy, HC are predominantly inactive in basal conditions (Giaume et al., 2010).

Astrocytes do not fire or propagate action potentials along their processes. Instead, they generate Ca^{2+} waves, consisting of increases in intracellular Ca^{2+} concentration ($[Ca^{2+}]_i$), that propagate along the astroglial network, triggering the release of gliotransmitters. These $[Ca^{2+}]_i$ increases usually involve the activation of G_q protein-coupled receptors, mainly ATP-operated P_2Y_1R (reviewed in Scemes et al., 2006, Giaume et al., 2010 and Agostinho et al., 2020). Additionally, astrocytic Ca^{2+} waves also appear to have a key role in blood flow control, since the production of vasoactive molecules is Ca^{2+}-dependent. Indeed, connexin expression is increased in astrocytic endfeet that enwrap blood vessels (*e.g.*, Rouach et al., 2008), enhancing perivascular propagation of Ca^{2+} waves (Giaume et al., 2010).

Importantly, astrocytes are strategically located between blood vessels and neurons, coupling neuronal activity to the supply of metabolic substrates, the so-called neurovascular coupling. This involves: 1) glutamate release by neurons, 2) Na^{+}-mediated glutamate uptake by astrocytes, 3) activation of the Na^{+}/K^{+}-ATPase that triggers blood glucose uptake and its glycolysis by astrocytes, and 4) lactate release by astrocytes that is used by neurons to meet their energy demand (reviewed in Giaume et al., 2010). In this model, known as astrocyte-neuron lactate shuttle, astrocytes are considered as individual entities. However, glutamate released from neurons can generate Na^{+}-mediated metabolic waves (*e.g.*, Bernardinelli et al., 2004), resulting in coordinated glucose uptake along the astroglial network (Giaume et al., 2010). In addition to glucose uptake, glutamate released from neurons also stimulates glucose trafficking along the astroglial network (*e.g.*, Rouach et al.,

2008), allowing an efficient supply of metabolites to remote sites of high neuronal energy demand (Giaume et al., 2010).

2.1. Astrocytic gap junction channels and hemichannels in Alzheimer's disease

Alterations in the expression and function of the astroglial GJC and HC protein Cx43 have increasingly been associated with neurotoxicity in AD. One of the pioneering studies reported that, in AD post-mortem cortical samples, areas enriched in Aβ plaques exhibit increased Cx43 immunostaining, and some sites of intensified Cx43 labeling colocalize with Aβ plaques (Nagy et al., 1996). In another study, the immunoreactivity and density of both Cx30 and Cx43, the two main astroglial connexins, were analyzed in the cortex and hippocampus from two different lines of APP/PS1 mice, the $APP_{SL}/PS1_{M146L}$ and $APP_{swe}/PS1_{dE9}$ mice (Mei et al., 2010). Accordingly, in young (2 months old) APP/PS1 mice, before the emergence of Aβ plaques, the distribution of both connexins is similar to that of WT mice. In older (≥ 4 months old) APP/PS1 mice, a higher immunoreactivity is detected for both connexins in reactive astrocytes associated with most Aβ plaques, contributing to the overall increase in connexin levels observed in aged (18 months old) APP/PS1 mice (Mei et al., 2010).

Differently, through an *in silico* approach, it was developed a network model that identifies subnetworks (modules) of co-expressed genes in late onset AD. One of those modules, called the khaki module, is highly enriched in astrocyte-specific genes, namely *APOE* (the main risk factor gene for sporadic AD, known to mediate Aβ clearance) and *GJA1* (the Cx43 encoding gene), the latter being predicted as the prominent regulator of this module (Zhang et al., 2013). In a subsequent study of the same group, *GJA1* expression was assessed across several gene expression datasets from post-mortem AD and control brains, demonstrating that *GJA1* is strongly correlated with AD pathogenesis, dementia and many AD risk factor genes (Kajiwara et al., 2018). Furthermore, in *GJA1* KO *versus* WT astrocytes co-cultured or not with WT neurons and exposed to synthetic $A\beta_{1-42}$ peptides, RNA sequencing analysis identified numerous differentially expressed genes, which significantly overlapped the khaki module. Cultured astrocytes lacking *GJA1* exhibit a reduction in *APOE* expression and density relatively to WT astrocytes. Additionally, WT neurons co-cultured with *GJA1* KO astrocytes display increased survival and viability upon $A\beta_{1-42}$ challenge than those co-cultured with WT astrocytes (Kajiwara et al., 2018).

Despite the discrepancy of results found in the literature, Aβ appears to have no effect on astrocytic GJ communication *in vivo* (*e.g.*, Cruz et al., 2010). Recently, Yi and colleagues used fluorescence recovery after photobleaching (FRAP) to measure cell-to-cell exchange of sulforhodamine 101 (SR101), a fluorescent tracer that is specifically taken up by astrocytes and passes through GJC. The kinetics of fluorescence recovery in photobleached hippocampal astrocytes is similar in old (9 months old) APP/PS1 and WT mice, indicating that astrocytic GJ communication is maintained in the hippocampus of APP/PS1 mice (Yi et al., 2016). In addition to astrocytic GJ communication, the same authors also evaluated astrocytic HC activity. Accordingly, APP/PS1 mice exhibit an increase in the signal of ethidium bromide (EtBr), a fluorescent tracer that passes through HC, relatively to WT mice, mainly in "close" (contacting Aβ plaques) astrocytes and to a lesser extent in "far" (distant from Aβ plaques) astrocytes. Carbenoxolone (CBX), a GJC and HC inhibitor, decreases the EtBr signal of APP/PS1 mice to the level of WT mice, in which CBX has no effect, confirming astrocytic HC activation in APP/PS1 mice (Yi et al., 2016).

Although the present study is centered on astrocytes, where connexin channels are most abundant ensuring astrocytic network organization, the expression and function of hemichannels is modified not only in astrocytes, but also in other brain cells, namely microglia and neurons, under AD-like conditions. Indeed, Aβ-induced HC activation was previously validated *in vitro*, in specific in cultured astrocytes, microglia and neurons. In accordance, these cell types were treated with synthetic $A\beta_{25-35}$ peptides, and the EtBr uptake assay, as well as whole-cell patch clamp recordings, were performed, revealing an increased HC activity in all three cell types, with microglia being most sensitive to Aβ treatment, then astrocytes and finally neurons (Orellana et al., 2011). In order to discriminate between Cx and Panx HC contribution to the overall HC activity, the EtBr uptake assay may be performed in the presence of specific HC inhibitors (for Cx HC, lanthanum trichloride ($LaCl_3$ or La^{3+}) and Cx43 mimetic peptides, such as Gap26; and for Panx HC, probenecid and Panx1 mimetic peptides, such as ^{10}Panx1). In this regard, it was found that Cx43 and Panx1 HC are activated in microglia, and the prominent contributors in astrocytes are Cx43 HC, whereas in neurons are Cx36 and Panx1 HC (Orellana et al., 2011). In turn, in hippocampal astrocytes from APP/PS1 mice, it was observed that Cx43 HC are the major contributors to the overall HC activity, but Panx1 HC may also have a smaller influence restricted to astrocytes contacting Aβ plaques. Noteworthy, EtBr uptake

in hippocampal astrocytes from APP/PS1-Cx30 KO mice is similar to that of age-matched control APP/PS1 mice, demonstrating that astrocytic Cx30 HC are not activated in APP/PS1 mice (Yi et al., 2016).

Distinct mechanisms are involved in Cx and Panx HC activation. As evaluated in hippocampal astrocytes from APP/PS1 mice, inflammation triggers Panx1 HC, while high $[Ca^{2+}]_i$ activates Cx43 HC, which also allow Ca^{2+} influx, sustaining high $[Ca^{2+}]_i$. In turn, activated Cx43 HC mediate the release of gliotransmitters, namely ATP and glutamate, which may also contribute to maintain high $[Ca^{2+}]_i$ through activation of purinergic and glutamatergic receptors (Yi et al., 2016). Since gliotransmitter release may be neurotoxic, neuronal oxidative stress and neuritic dystrophy, two parameters reflecting neuronal damage, were examined in APP/PS1-Cx43 KO mice and age-matched control APP/PS1 mice. In accordance, it was shown that the knockout of Cx43 in astrocytes prevents neuronal oxidative stress and neuritic dystrophy, suggesting that the suppression of astrocytic Cx43 HC activity may represent an alternative valuable therapeutic strategy in AD (Yi et al., 2016).

Interestingly, Orellana and colleagues demonstrated that Aβ-induced glial (microglia and astrocytes) HC activation increases the activity of neuronal HC, promoting neuronal death. Briefly, neuronal cultures exposed to conditioned medium from either microglial or astrocytic cultures treated with $A\beta_{25-35}$ display increased EtBr uptake and Fluoro-Jade C, a marker of neuronal death, positive cells relatively to control cultured neurons. The absence of these effects on cultured neurons exposed only to $A\beta_{25-35}$ indicates that they do not depend on Aβ treatment, but rather on glial HC activation. Noteworthy, Cx and Panx HC inhibitors, as well as antagonists of purinergic and glutamatergic receptors, P_2X_7R and NMDAR respectively, counteract neuronal HC activation and death. Similar results were obtained from mouse hippocampal slices exposed to $A\beta_{25-35}$ (Orellana et al., 2011).

3. Adenosine receptors: A branch of the purinergic system

ATP consists of an adenine-based purine attached to a ribose (collectively referred to as adenosine) and a triphosphate group (originating adenosine triphosphate, ATP), and it is best known as the main cell energy source, although ATP (acting on purinergic P_2R) and adenosine (acting on purinergic P_1R) can also function as extracellular signals, defining the purinergic system (reviewed in Agostinho et al., 2020). Accordingly, ATP can be released

through Ca^{2+}-dependent exocytosis, as well as connexin or pannexin channels. ATP signaling involves rapid responses mediated by ionotropic P_2XR, of which there are seven subunits ($P_2X_{1-7}R$) forming homo or heteroreceptors, as well as slower responses operated by eight G protein-coupled P_2YR ($P_2Y_{1,2,4,6,11-14}R$) (Agostinho et al., 2020). In turn, extracellular levels of adenosine are regulated via AMP dephosphorylation, the last and rate-limiting step of the enzymatic breakdown of extracellular ATP, through the action of ecto-nucleotidases, in particular ecto-5′-nucleotidase (CD73). Additionally, adenosine can also be released directly via equilibrative nucleoside transporters (ENT), namely ENT-1, which can also take up adenosine. Although adenosine can operate four G protein-coupled P_1R: A_1R, $A_{2A}R$, $A_{2B}R$ and A_3R, adenosine signaling in the brain is primarily operated by inhibitory A_1R (coupled to G_i protein, decreasing cAMP levels) and facilitatory $A_{2A}R$ (coupled to G_s protein, increasing cAMP levels) (Agostinho et al., 2020).

In general, there is a greater advance in understanding the role of adenosine signaling, rather than ATP signaling, in the brain. Both A_1R and $A_{2A}R$ are concentrated in glutamatergic synapses, although $A_{2A}R$ density is several-fold lower than A_1R, and perhaps the most important role of the interplay between these receptors is to sharpen information salience encoding (reviewed in Cunha et al., 2016 and Agostinho et al., 2020). In this context, under low intensity/frequency of information flow, there is a predominant A_1R-mediated inhibition of synaptic transmission. When relevant information is to be encoded, there is a local burst of ATP release, which is converted into adenosine activating $A_{2A}R$. In turn, $A_{2A}R$ enhance synaptic plasticity by shutting down A_1R (*e.g.*, Ciruela et al., 2006) and enhancing NMDAR activity (*e.g.*, Rebola et al., 2008). In parallel, recruitment of the astrocytic syncytium increases extracellular levels of adenosine, enhancing A_1R-mediated inhibition in all synapses except in the "activated" synapse, a process called heterosynaptic depression (*e.g.*, Andersson et al., 2007).

The two major adenosine receptors also appear to have different roles on neurodegeneration (reviewed in Cunha et al., 2016 and Agostinho et al., 2020). In accordance, brain insults lead to a surge of extracellular ATP, considered as a danger signal in the brain, and ATP-derived adenosine. The initial increase in extracellular levels of adenosine preferentially activates A_1R, which act as a hurdle to preserve neuronal function, to what is called preconditioning (*e.g.*, Fedele et al., 2006 revealing that A_1R activation prevents seizure progression). However, when extracellular adenosine increases to levels that supra-maximally activate A_1R, these receptors desensitize and the hurdle is overcome.

Then, $A_{2A}R$ are activated and the damage spreads throughout the brain (*e.g.*, Li et al., 2015; Pagnussat et al., 2015; Temido-Ferreira et al., 2020 reporting that $A_{2A}R$ activation is sufficient to trigger memory impairment).

3.1. Adenosine A_{2A} receptors in Alzheimer's disease

$A_{2A}R$ are mainly located in striatum, where they play an important role in motor control. However, in AD, there is a redistribution of these receptors, appearing in frontal cortex and hippocampus, which are brain regions relevant to mnemonic and cognitive functions (*e.g.*, Angulo et al., 2003; Albasanz et al., 2008). Accordingly, a recent study showed, through a binding assay using the selective $A_{2A}R$ antagonist [^{3}H]ZM 241385 as radioligand, that AD patients exhibit an increase in $A_{2A}R$ density in frontal white and gray matter, as well as in hippocampus/entorhinal cortex, relatively to age-matched control subjects. The levels of $A_{2A}R$ in hippocampus/entorhinal cortex are also higher than in frontal white and gray matter in AD patients, whereas there is no difference between these brain regions in control subjects. Thus, $A_{2A}R$ expression seems to mirror AD progression, from hippocampus/entorhinal cortex, where the pathology is more pronounced, to other cortical brain areas (Merighi et al., 2021). Moreover, the same study also reported that $A_{2A}R$ density is higher in platelets (a blood cell type, considered as the main Aβ source in circulation) from AD patients than those from control subjects, suggesting that $A_{2A}R$ from platelets may be a peripheral AD marker, since they reflect the upregulation of $A_{2A}R$ observed at the central level (Merighi et al., 2021).

The widely reported upregulation of $A_{2A}R$ upon perturbation of brain function, as in AD, raised the hypothesis that $A_{2A}R$ overactivation may be a cause for memory impairment. Indeed, it was already shown that the pharmacological activation of $A_{2A}R$, through intraperitoneal or intracerebroventricular injection of the selective $A_{2A}R$ agonist CGS 21680, is sufficient to trigger memory deficits in mice (Pagnussat et al., 2015). Likewise, the optogenetic activation of mouse hippocampal $A_{2A}R$ is sufficient to recruit the cAMP/PKA-mediated c-Fos/phospho-CREB pathway and impair memory (Li et al., 2015). Taken together, these findings point out a promising role in counteracting $A_{2A}R$ overactivation to manage AD, as it will be reviewed below.

Accumulating evidences support a protective role of non-toxic doses of caffeine, whose only known molecular targets are adenosine receptors, against AD. Caffeine

consumption appears, in fact, to inversely correlate with the incidence of AD (Maia and de Mendonça, 2002). In particular, Eskelinen and colleagues reported that moderate coffee drinkers (3-5 cups of coffee per day) at midlife have a reduced risk of dementia and AD at late-life, compared to those who drink no or little coffee. Tea drinking, which was uncommon in the study population, making statistical power low, has no association with dementia/AD, probably due to a low caffeine content in tea (Eskelinen et al., 2009). However, using humans to assess whether caffeine consumption protects against AD has some limitations, namely: 1) retrospective studies are based on recall and cannot unequivocally isolate caffeine from other factors, and 2) prospective (longitudinal) studies involving caffeine administration over decades are impractical. Thus, in order to address this key question, controlled *in vitro* and *in vivo* studies have emerged (*e.g.*, Dall'Igna et al., 2003; Arendash et al., 2006; Dall'Igna et al., 2007; Arendash et al., 2009).

The extent to which adenosine receptor antagonism is involved in the mechanisms of caffeine action to protect against AD has been largely explored. Dall'Igna and colleagues reported, for the first time, that the application of either caffeine or the selective $A_{2A}R$ antagonist ZM 241385, but not the adenosine receptor antagonist 8-cyclopentyltheophylline which, at the concentration used, functions as A_1R antagonist, prevents neuronal death caused by exposure of rat cerebellar neuron cultures to synthetic $A\beta_{25-35}$ peptides (Dall'Igna et al., 2003). In a subsequent *in vivo* study of the same authors, it was observed that, in mice injected intracerebroventricularly with $A\beta_{25-35}$, the subchronic treatment with either caffeine or the selective $A_{2A}R$ antagonist SCH 58261, consisting of a single intraperitoneal injection of one of these drugs daily for few days, prevents $A\beta_{25-35}$-induced cognitive impairment (Dall'Igna et al., 2007). Collectively, the results from both studies indicate that the pharmacological blockade of $A_{2A}R$, but not of A_1R, mimics the neuroprotective effect of caffeine against Aβ-induced neurotoxicity and memory impairment, suggesting that $A_{2A}R$ may be the molecular target responsible for the reported beneficial effect of caffeine consumption in AD.

An insightful study proved that the effectiveness of $A_{2A}R$ blockade does not extend to all conditions involving memory impairment, but it is specifically pertinent in conditions where synaptic dysfunction occurs, namely AD. In accordance, the intracerebroventricular injection of synthetic $A\beta_{1-42}$ peptides in rats decreases memory performance to an extent similar to that caused by the intraperitoneal injection of either scopolamine (a non-selective muscarinic receptor antagonist) or MK 801 (dizocilpine, a

NMDAR antagonist). However, the pharmacological blockade of $A_{2A}R$, through intraperitoneal injection of the selective $A_{2A}R$ antagonists SCH 58261 or KW 6002 (istradefylline), prevents $A\beta_{1-42}$-induced, but not scopolamine- or MK 801-induced, amnesia (Cunha et al., 2008). Indeed, the intracerebroventricular injection of $A\beta_{1-42}$ is considered a model of early AD, since it recapitulates the two main features associated with the onset of AD, that is, synaptic dysfunction and memory impairment, rather than Aβ deposition, neuronal damage, astrogliosis or microgliosis, which occur at late stages of AD. Additionally, these $A\beta_{1-42}$-induced effects can be prevented by both the pharmacological blockade and the knockout of $A_{2A}R$ (Canas et al., 2009). Therefore, the disruption of $A_{2A}R$ activity seems to be only effective when the leading cause for memory deficits is synaptic dysfunction (as upon Aβ administration), and not the transient blockade of certain transducing systems (as upon scopolamine or MK 801 administration).

Although the first idea that comes to mind is that $A_{2A}R$ signal through activation of the cAMP/PKA pathway, they are actually pleiotropic receptors, engaging many transducing systems, as supported by the observation that $A_{2A}R$ blockade decreases long-term potentiation (LTP) in basal conditions, whereas it is increased upon different brain insults, including Aβ exposure. In this regard, it was observed, specifically in the hippocampus, that $A_{2A}R$ recruit the cAMP/PKA-mediated c-Fos/phospho-CREB pathway to control memory performance in basal conditions (Li et al., 2015), while they signal through a p38 MAPK-dependent pathway to afford neuroprotection against Aβ-induced neurotoxicity and memory impairment (Canas et al., 2009).

It is worth noting that the studies reviewed above point out that the beneficial effect of caffeine consumption in AD may be due to caffeine-mediated $A_{2A}R$ blockade. However, they do not exclude the possibility that other mechanisms may be involved. In particular, Arendash and colleagues demonstrated that long-term administration of a moderate amount of caffeine (the human equivalent of 5 cups of coffee, or 500 mg of caffeine, per day) in the drinking water protects young-adult APP_{sw} mice against cognitive impairment in older age (Arendash et al., 2006), as well as reverses already present cognitive impairment in aged APP_{sw} mice (Arendash et al., 2009). These beneficial effects of caffeine on cognition are accompanied by a decrease in soluble/deposited brain Aβ levels through a reduction of Aβ production (Arendash et al., 2006; Arendash et al., 2009). Indeed, they observed that the hippocampal expression of

both BACE1 (the most enzymatically active BACE variant) and PS1 (the catalytic subunit of the γ-secretase complex) is reduced in caffeine-treated APP_{sw} mice (Arendash et al., 2006). Possible mechanisms involved in this caffeine-mediated suppression of BACE1 and PS1/γ-secretase expression were also unraveled, by showing that: 1) caffeine stimulates PKA activity, which underlies the observed increase in inactive cRaf-1 levels in the hippocampus of APP_{sw} mice, suppressing NFκB activity and the expression of NFκB-controlled genes, such as BACE1, and 2) caffeine reduces the levels of both α and β isoforms of GSK3 in SweAPP N2a cells, decreasing PS1/γ-secretase activity and increasing tau hyperphosphorylation, respectively (Arendash et al., 2009).

3.1.1. Astrocytic adenosine A_{2A} receptors

Accumulating evidences support that $A_{2A}R$ may operate different mechanisms at different stages of AD to control memory impairment, with a role for synaptic $A_{2A}R$ at early stages (as mentioned above) and astrocytic $A_{2A}R$ at late stages. The last evidence was reported, for instance, by Orr and colleagues, who showed that AD patients and aged hAPP mice (plaque-bearing), but not young hAPP mice, have increased astrocytic $A_{2A}R$ levels in the hippocampus. Additionally, genetic deletion of astrocytic $A_{2A}R$ in aged hAPP mice, but not in young hAPP mice, enhances memory (Orr et al., 2015).

One of the utmost functions ensured by astrocytes is the uptake of glutamate from the synaptic cleft, whose extracellular accumulation would lead to excitotoxic neuronal death. Accordingly, Matos and colleagues investigated whether astrocytic $A_{2A}R$ regulate glutamate uptake in non-pathological conditions, and they observed that acute exposure of primary cultured cortical astrocytes and cortical gliosomes (purified membranes from astrocytic processes) to the selective $A_{2A}R$ agonist CGS 21680 decreases D-aspartate (substrate for glutamate transporters) uptake, which is prevented by the selective $A_{2A}R$ antagonist SCH 58261 (Matos et al., 2012a). In addition, they demonstrated that this astrocytic $A_{2A}R$-mediated control of glutamate uptake is dependent of the cAMP/PKA signaling pathway, since both SCH 58261 and the PKA inhibitor H89 prevent the decrease in D-aspartate uptake and expression of the astrocytic glutamate transporters GLAST (human homologue EAAT1) and GLT1 (human homologue EAAT2) caused by prolonged exposure of cultured astrocytes to CGS 21680 (Matos et al., 2012a).

Subsequently, Matos and colleagues hypothesized that astrocytic $A_{2A}R$-mediated control of glutamate uptake might be involved in the neuroprotection afforded by $A_{2A}R$ blockade against Aβ-induced neurotoxicity. Thus, they reported later that, in primary cultured cortical astrocytes, $A\beta_{1-42}$ decreases D-aspartate uptake, an effect abolished upon pharmacological blockade or genetic deletion of $A_{2A}R$. Furthermore, $A\beta_{1-42}$ decreases the expression of the glutamate transporters GLAST and GLT1 in cultured astrocytes from WT, but not from global $A_{2A}R$ KO mice (Matos et al., 2012b). Interestingly, the partial loss of the glutamate transporter GLT1 in an AD mouse model ($GLT1^{+/-}$ mice crossed with transgenic APP/PS1 mice) accelerates the onset of cognitive deficits (Mookherjee et al., 2011). Moreover, a recent study from our group showed that $A_{2A}R$ regulate Ca^{2+} dynamics mediated by ATP-operated P_2X_7R and P_2Y_1R in cultured astrocytes, being the interplay between these receptors disrupted upon $A\beta_{1-42}$ challenge (Dias et al., 2022).

Recently, new insights about the role of astrocytic $A_{2A}R$ were provided by resorting to an *in silico* approach. In accordance, it was demonstrated that $A_{2A}R$ overexpression promotes transcriptional deregulation in cultured astrocytes, mainly affecting genes related to immune responses, angiogenesis and gliosis. Treatment with the selective $A_{2A}R$ antagonist SCH 58261 is able to restore the expression levels of these genes (Paiva et al., 2019).

CHAPTER II

Aims

Recently, our group demonstrated that $A\beta_{1-42}$ exposure: 1) triggers ATP release through Cx43 HC, 2) increases Cx43 HC activity, and 3) leads to Cx43 upregulation and phosphorylation in primary astrocyte cultures, and that these effects are prevented by both selective $A_{2A}R$ antagonism and inhibition of CD73-mediated adenosine formation. Overall, these data identified a vicious circle occurring in cultured astrocytes exposed to $A\beta_{1-42}$, whereby $A_{2A}R$ regulate Cx43 HC activity, leading to increased ATP release, which is converted into adenosine by CD73, overactivating $A_{2A}R$ (Madeira et al., 2021). However, it is worth noting that our previous observations derived solely from *in vitro* studies and remain to be confirmed in a more integrated biological system, where neuronal, glial and vascular interactions are present.

The major goal of the present study was to investigate the putative $A_{2A}R$-mediated regulation of astrocytic Cx43 HC activity in non-pathological and AD-like conditions. To achieve this goal, we used brain slices from the mouse hippocampus, a brain structure critical for spatial memory that is particularly affected in AD. Furthermore, this work was also important to optimize an EtBr uptake assay, with EtBr being a fluorescent tracer that passes through HC and accumulates in cell nuclei, as well as to implement a three-dimensional image processing and analysis protocol for quantification of EtBr fluorescence intensity per astrocyte (GFAP immuno-positive) nucleus volume, which represented our index of astrocytic EtBr uptake and, hence, HC activity. Indeed, analyzing the multi-slice stack (3D image), instead of overlapping the slices in a 2D image, allows the nuclei to be more individualized, making quantification more accurate.

Initially, to examine whether astrocytic Cx43 HC activity is affected under AD-like conditions, we used hippocampal slices superfused with synthetic $A\beta_{1-42}$ peptides, and then we evolved to AD mouse models, namely mice injected intracerebroventricularly with $A\beta_{1-42}$ recapitulating sporadic AD, and APP/PS1 transgenic mice modeling familial AD. Moreover, to infer about the impact of $A_{2A}R$ on astrocytic Cx43 HC activity, we resorted to both pharmacological and genetic tools, including a selective $A_{2A}R$ antagonist (SCH

58261) and a CD73 inhibitor (AOPCP), as well as transgenic mice with global $A_{2A}R$ gene deletion. Additionally, we used a viral transgenic construct to specifically silence $A_{2A}R$ in astrocytes. We also used transgenic mice with neuron-specific $A_{2A}R$ gene deletion, and evaluated whether neuronal, in addition to astrocytic, $A_{2A}R$ regulate astrocytic Cx43 HC activity upon $A\beta_{1-42}$ challenge.

CHAPTER III

Materials and methods

1. Animals

Animals were housed in cages, with *ad libitum* access to food and water, under a controlled environment with 23 ± 2°C temperature, approximately 66% humidity and fixed 12h dark/light cycle. Experiments were approved by the ethical committees of the institution (*Órgão Responsável pelo Bem-Estar dos Animais* (ORBEA), 128_2015/04122015) and Portugal (*Direção Geral de Alimentação e Veterinária* (DGAV), 0421/000/000/2016 Ref 014420), and conducted in accordance with European legislation on animal welfare. The animals used in this study were: 1) mice with global, neuron- or astrocyte-specific $A_{2A}R$ gene deletion, 2) C57 black 6 (C57BL/6) mice injected intracerebroventricularly (icv) with either $A\beta_{1-42}$ or vehicle, and 3) APP/PS1 mice, which are characterized below.

1.1. $A_{2A}R$ gene-deleted mice

Mice with global and neuron-specific $A_{2A}R$ gene deletion: Global $A_{2A}R$ knockout (Gb-$A_{2A}R$ KO) and forebrain neuron $A_{2A}R$ knockout (Fb-$A_{2A}R$ KO) mice, both with C57BL/6 genetic background, were generated in Jiang-Fan Chen's lab (Boston University School of Medicine, Boston, Massachusetts), as described in Chen et al., 1999 and Bastia et al., 2005, respectively. These mice were generously provided to our group and have been reproduced at our institution's animal core facility.

Mice with astrocyte-specific $A_{2A}R$ gene deletion: These mice were generated taking advantage of the Cre/loxP system through a viral transgenic construct (see Figure 5C). This system requires the use of transgenic mice with the gene of interest ($A_{2A}R$ gene) flanked by two loxP sequences, referred to as floxed gene ($A_{2A}R^{fl/fl}$ gene). These loxP sequences are recognized by Cre recombinase (or simply Cre), an enzyme that is not normally expressed in mouse brain cells, excising the floxed gene. Both Cre and green fluorescent

protein (GFP), the latter functioning as an infection reporter, were placed under the control of glial fibrillary acidic protein (GFAP) transcription promoter, which is astrocyte-specific. Adeno-associated virus serotype 5 (AAV5) was chosen since it has higher astrocyte transduction efficiency compared with other serotypes, as assessed in spinal cord astrocytes (Griffin et al., 2019).

In accordance, Fb-A_{2A}R mice, which carry floxed A_{2A}R gene, were injected into the left and right dorsal hippocampi with AAV5/GFAP-GFP-Cre (4.8×10^9 mol in 1 μL; Gene Therapy Center – Vector Core Facility, University of North Carolina School of Medicine, Chapel Hill, North Carolina). After deep anesthesia with isoflurane (IsoVet – B. Braun, Lisbon, Portugal), mice were placed in a stereotaxic apparatus, and their skulls were drilled for viral vector infusion. The stereotaxic coordinates for virus administration, defined relatively to bregma (intersection between the sagittal and coronal skull sutures), were the following: anteroposterior (AP): -2.00 mm, mediolateral (ML): ±1.60 mm and dorsoventral (DV): -1.60 mm, which correspond to the hippocampal CA1 region. These mice were used in the experiments 1 month after surgery, a time point sufficient to attain robust transgene transduction (Lopes and Madeira et al., 2022). In all experiments, 3-month-old male and female mice with A_{2A}R gene deletion (either global, neuron- or astrocyte-specific) and age-matched control mice were used.

1.2. icv-Aβ_{1-42} mice

Female C57BL/6 mice (Charles River Laboratories, Barcelona, Spain) with 6 weeks old were deeply anesthetized with avertin solution (in mM: 70.7 2,2,2-tribromoethanol and 450 2-methyl-2-butanol) in phosphate buffered saline (PBS; in mM: 137 NaCl, 2.7 KCl, 10 Na_2HPO_4 and 1.9 KH_2PO_4, at pH 7.4). Then, mice were subjected to a stereotaxic surgery for icv injection of either Aβ_{1-42} (2 nmol in 4 μL; Bachem, Bubendorf, Switzerland) or vehicle (4 μL water). More precisely, the injection was directed to the left lateral ventricle (stereotaxic coordinates from bregma, in mm: AP: -0.58, ML: ±1.13 and DV: -2.00). These mice were used in the experiments 2 weeks after surgery, a time point previously validated by us. Indeed, this mouse model of sporadic AD has been extensively used by our group, demonstrating that the Aβ_{1-42} solution used (2.25 mg/mL) is mostly composed of Aβ oligomers, and icv-Aβ_{1-42} mice display within 2 weeks an impairment of spatial reference

memory and synaptic plasticity, as well as loss of synaptic markers (*e.g.*, Canas et al., 2009; Lopes et al., 2022).

1.3. APP/PS1 mice

Male $APP_{swe}/PS1_{dE9}$ (or simply APP/PS1) mice with B6C3F1/J genetic background (Jackson Laboratory, Bar Harbor, Maine) with 9 months of age and WT littermates were used in the experiments. Serving as a model for familial AD, these double transgenic mice express chimeric mouse/human APP 695 with the Swedish (K595N/M596L) mutations, along with human PS1 carrying the exon-9-deleted (dE9) mutation, specifically in neurons (*https://www.jax.org/strain/005864*). These mice are characterized by an impairment of spatial working and reference memory starting at ≈6 months old and aggravating at older ages, presence of Aβ plaques in the brain as early as 3 months old, as well as an increase in brain Aβ levels *versus* a decrease in plasma Aβ levels with advancing age (*e.g.*, Izco et al., 2014). It is worth mentioning that our group also detected deficits of spatial memory in 9-month-old APP/PS1 mice compared to WT littermates (unpublished data yet).

2. Hippocampal slices

Mice were sacrificed by decapitation after deep anesthesia with halothane (Sigma-Aldrich, St. Louis, Missouri). The brain was removed and the hippocampus dissected in gassed (95% O_2 and 5% CO_2) ice-cold artificial cerebrospinal fluid (ACSF; in mM: 124 NaCl, 3 KCl, 1.25 NaH_2PO_4, 26 $NaHCO_3$, 10 glucose, 1 $MgSO_4$ and 2 $CaCl_2$, at pH 7.4), in order to slow down metabolic activity and prevent cell damage. Transversal hippocampal slices (400-μm-thick) were prepared using a McIlwain tissue chopper, and then recovered functional and energetically in gassed ACSF for 90 min at a near-physiological temperature of 32°C, in order to prevent excitotoxic cell death. Afterward, the slices were kept at room temperature (RT).

3. Pharmacological treatments

Control hippocampal slices were only exposed to ACSF. $A\beta_{1-42}$-treated hippocampal slices were incubated with $A\beta_{1-42}$ (1 μM; Bachem) diluted in gassed ACSF for 60 min at RT. The effect of selective $A_{2A}R$ antagonism on $A\beta_{1-42}$-treated hippocampal slices was tested by incubating the slices with SCH 58261 (50 nM; Tocris Bioscience, Bristol, England) 30 min prior to $A\beta_{1-42}$ challenge. When testing the effect of selective $A_{2A}R$ antagonism, as well as CD73 and Cx43 HC inhibition, in AD mouse models, the hippocampal slices were incubated with SCH 58261, AOPCP (100 μM; Tocris Bioscience) and Gap19 (250 μM; Tocris Bioscience) in gassed ACSF for 90 min at RT, respectively.

4. Ethidium bromide uptake assay

HC activity was evaluated through the uptake of ethidium bromide (EtBr), a nucleic acid-intercalating agent that passes through HC and fluoresces once bound to DNA. The higher EtBr signal fluorescence intensity, the higher EtBr uptake and, hence, HC activity (Giaume et al., 2012). Following pharmacological treatments, the hippocampal slices were incubated with EtBr (20 μM; Sigma-Aldrich) diluted in gassed ACSF for 5 min at RT. Then, the slices were rinsed in gassed ACSF for 15 min at a low temperature (rinsing chamber on ice), in order to stop EtBr uptake and reduce background fluorescence. Afterward, the slices were fixed by immersion in 4% paraformaldehyde (PFA) in PBS overnight at 4°C, in order to preserve tissue structure. Since increasing fixation time may increase background fluorescence, the slices were transferred to PBS, and then stored at 4°C until immunohistochemical processing.

5. Immunohistochemistry

After performing the EtBr uptake assay, the hippocampal sections were immunohistochemically processed to label GFAP, a classic astrocytic marker. The sections were washed with glycine solution (500 mM glycine in PBS) for 5 min, in order to quench residual paraformaldehyde. This was followed by three 10 min washes with glycine solution whose concentration was successively halved, and then the sections were washed with PBS for five times 10 min each. Next, the sections were incubated with

permeabilization solution (0.1% Triton X-100 (Sigma-Aldrich) in PBS) for 30 min at RT to facilitate cell entry of the primary antibody, and then with blocking solution (10% horse serum (HS; Thermo Fisher Scientific, Waltham, Massachusetts) in permeabilization solution) for 2h at RT to block unspecific binding. The sections were posteriorly incubated with rabbit polyclonal anti-GFAP primary antibody (1:1000; Millipore, Billerica, Massachusetts) diluted in blocking solution for 2 days at 4°C. After incubating twice with permeabilization solution for 10 min and once with blocking solution for 30 min at RT, the sections were incubated with donkey anti-rabbit Alexa Fluor 488 secondary antibody (1:500; Thermo Fisher Scientific) diluted in blocking solution for 4h at RT. Exclusively for mice with $A_{2A}R$ gene deletion in astrocytes, which express GFP, the sections were incubated with goat polyclonal anti-GFP primary antibody (1:500; Abcam, Cambridge, England) and donkey anti-goat Alexa Fluor 488 secondary antibody (1:500; Thermo Fisher Scientific) to enhance GFP fluorescence signal, and GFAP secondary antibody was instead goat anti-rabbit Alexa Fluor 647 (1:500; Thermo Fisher Scientific). Then, the hippocampal sections were washed with PBS for three times 20 min each, incubated with Hoechst 33258 (1:2000; Sigma-Aldrich) diluted in PBS for 30 min at RT to stain the nuclei, and washed again with PBS for three times 10 min each. Finally, the sections were mounted on chamber slides (Ibidi μ-slide 8 well treated; Ibidi, Gräfelfing, Germany), since in conventional slides the coverslips would crush the thicker sections used. The mounting medium was Fluoromount Aqueous Mounting Medium (Sigma-Aldrich) and, after drying at RT, the sections were stored at 4°C until image acquisition.

6. Imaging workflow

6.1. Acquisition

Hippocampal section immunostaining was detected using an inverted confocal laser scanning microscope, the Zeiss LSM 710 coupled to the computer software Zeiss Zen Software Black Edition 2012 (Zeiss, Oberkochen, Germany), with a Plan-Apochromat 40x/1.4 Oil DIC M27 objective. The laser lines used were Diode 405 nm (for excitation of Hoechst 33258 that emits blue fluorescence), Argon multiline 458, 488, 514 nm (for excitation of Alexa Fluor 488 dye that emits green fluorescence) and 561 nm (for excitation of EtBr that emits reddish-orange fluorescence). Exclusively for mice with $A_{2A}R$ gene deletion in astrocytes, the 633 nm laser line was used (for excitation of Alexa Fluor 647

dye that emits fluorescence on far-red). Each image consisted of a stack of optical sections taken through the Z-plane, referred to as Z-stack. Per hippocampal section, 2-3 images covering different areas of the hippocampal CA1 region were acquired. Per animal, 1-4 hippocampal sections were used in each experimental condition. Microscope settings were kept the same for all images where comparisons would be made.

6.2. Processing pipeline

Before quantification of EtBr fluorescence signal in astrocyte nuclei, images were: 1) pre-processed, to increase spatial resolution and signal-to-noise ratio, as well as to decrease background fluorescence, 2) segmented, to detect the nuclei, and 3) post-processed, to separate touching nuclei.

Microscopy images are distorted by physical processes (namely, diffraction and noise), which can be described by a mathematical operation named convolution. Basically, convolution replaces every point light source by its correspondent point spread function (PSF), producing a blurry image. The inverse operation, referred to as deconvolution, collects the spread light and puts it back to its original location, producing a more reliable image of the object (*https://svi.nl/Huygens-Deconvolution*). Therefore, images were deconvolved using Huygens Remote Manager, a multi-user, web-based interface to Huygens software, which performs deconvolution without changing intensity values. It requires the creation of two parameter templates, one for the imaging parameters and the other for the restoration parameters. Theoretical PSF and classic maximum likelihood estimation (CMLE) algorithm were used since they are accurate in most of the cases (*https://huygens-remote-manager.readthedocs.io/*).

When imaging thicker specimens (*e.g.*, 400 μm), there is a significant amount of background fluorescence, which can be managed with a normalization operation. Normalization of the intensities of each optical section, which consists of subtracting each intensity value from the mean and then dividing by the standard deviation, allows intensities to be within the same range (in other words, to be more homogeneous) and, concomitantly, to reduce background (Imaris 9.6 Reference Manual). The normalization function was applied to the GFAP channel, allowing to visualize and quantify more astrocytes, using the computer software Imaris 9.6.1 (Bitplane, Zürich, Switzerland), whose functionalities were also exploited in the subsequent processing steps and analysis.

For segmentation, *Surfaces* were created from the nuclei channel. The pre-selected *Smooth* option and default *Surfaces Detail* value were accepted. For thresholding, the *Background Subtraction* option was selected. This option applies a Gaussian filter to estimate the background of each voxel, and then subtracts each background value from each intensity value (Imaris 9.6 Reference Manual). The *Diameter of largest Sphere which fits into the Object* was set to 10 μm, an approximate value of the maximum measured nucleus diameter. In order to ensure reproducibility, the automatic threshold value (or a slight adjustment) was used. Finally, touching *Surfaces* were separated manually.

6.3. Analysis

EtBr fluorescence intensity measured in the nucleus (in arbitrary units, au) divided by the volume of the nucleus (in μm^3) was taken as an index of EtBr uptake for each hippocampal astrocyte. Not all $GFAP^+$ cells were considered, namely cells whose nucleus was cut in the X-, Y- or Z-plane, or undergoing mitosis. Additionally, cells whose nucleus exhibited EtBr fluorescence that blended with the background fluorescence ($EtBr^-$ cells), or excessively bright EtBr fluorescence (possibly, injured cells), were also not considered. It is worth mentioning that, for mice with $A_{2A}R$ gene deletion in astrocytes, only infected cells (GFP^+ cells) were quantified. Images were analyzed blindly to avoid potential bias.

7. Data presentation and statistical analysis

As already mentioned, for each hippocampal section, several images (2-3 images) covering different areas of the hippocampal CA1 region were taken. The outliers of each image, that is, the astrocytes that take up an abnormally high or low amount of EtBr, were detected using a rule that considers a value as an outlier if it is:

Greater than Q3 + 1.5 IQR

OR

Smaller than Q1 – 1.5 IQR

This rule is based on the boxplot representation of the data, and Q1 stands for the first quartile, Q3 the third quartile and IQR the interquartile range. After excluding the outliers, the mean for each image was determined. Then, the mean for each section was calculated by averaging the previous means. Finally, the response of each animal to a certain

experimental condition was calculated by averaging the means of all sections (1-4 sections) of that animal.

For the number (*n*) of independent experiments (experiments reproduced using different animals) indicated in figure captions, data were presented as *Mean* ± *Standard error of the mean (SEM)*. The response, that is, astrocytic EtBr uptake through HC, was studied under two variables: 1) AD-like conditions, and 2) specific protein activity ($A_{2A}R$, CD73 and Cx43). Hence, two-way analysis of variance (ANOVA), followed in case of significance by the recommended *post hoc* test, was performed. In order to highlight the effect of AD-like conditions on the response, experimental and control groups were graphed and, after confirming the normality assumption, *t*-test was performed. Within-subject (*e.g.*, treated *versus* non-treated APP/PS1 mice) statistically significant differences are indicated by $*p < 0.05$, $**p < 0.01$, $***p < 0.001$ and $****p < 0.0001$. Between-subject (*e.g.*, non-treated APP/PS1 *versus* WT mice) statistically significant differences are indicated by $\#p < 0.05$, $\#\#p < 0.01$, $\#\#\#p < 0.001$ and $\#\#\#\#p < 0.0001$. Graphical representation of the data and statistical analysis were performed using the computer software GraphPad Prism 8.0.1 (GraphPad, San Diego, California).

CHAPTER IV

Results

1. 3D image processing and analysis pipeline

The putative role of $A_{2A}R$ in the regulation of astrocytic Cx43 HC activity under AD-like conditions, consistent with our previous findings in primary astrocyte cultures exposed to $A\beta_{1-42}$ (Madeira et al., 2021), was here investigated in hippocampal slices, which represent a more integrated biological system, by performing the EtBr uptake assay. EtBr is a fluorescent tracer that passes through HC and accumulates in cell nuclei, so the higher EtBr uptake, the higher HC activity, as described in Giaume et al., 2012. Figure 1 depicts the image processing and analysis pipeline for quantification of EtBr fluorescence intensity per astrocyte nucleus volume, which included: 1) some pre-processing operations for better visualization of astrocytes (A-C), 2) segmentation of nuclei (D-E), and 3) selection of astrocyte nuclei (F-G). As detailed in the Materials and methods section, this pipeline was implemented using Imaris software, a graphical user interface highly suitable for working with 3D images. Indeed, in Imaris it is possible to analyze the Z-stack without having to overlap the optical sections. Additionally, under the Imaris *Surpass Object* of type *Surfaces*, there is a built-in function that allows to manually separate touching *Surfaces* (nuclei) and *Surfaces* volume is automatically computed. Overall, these were considered important features as compared to the "gold standard" software ImageJ/Fiji.

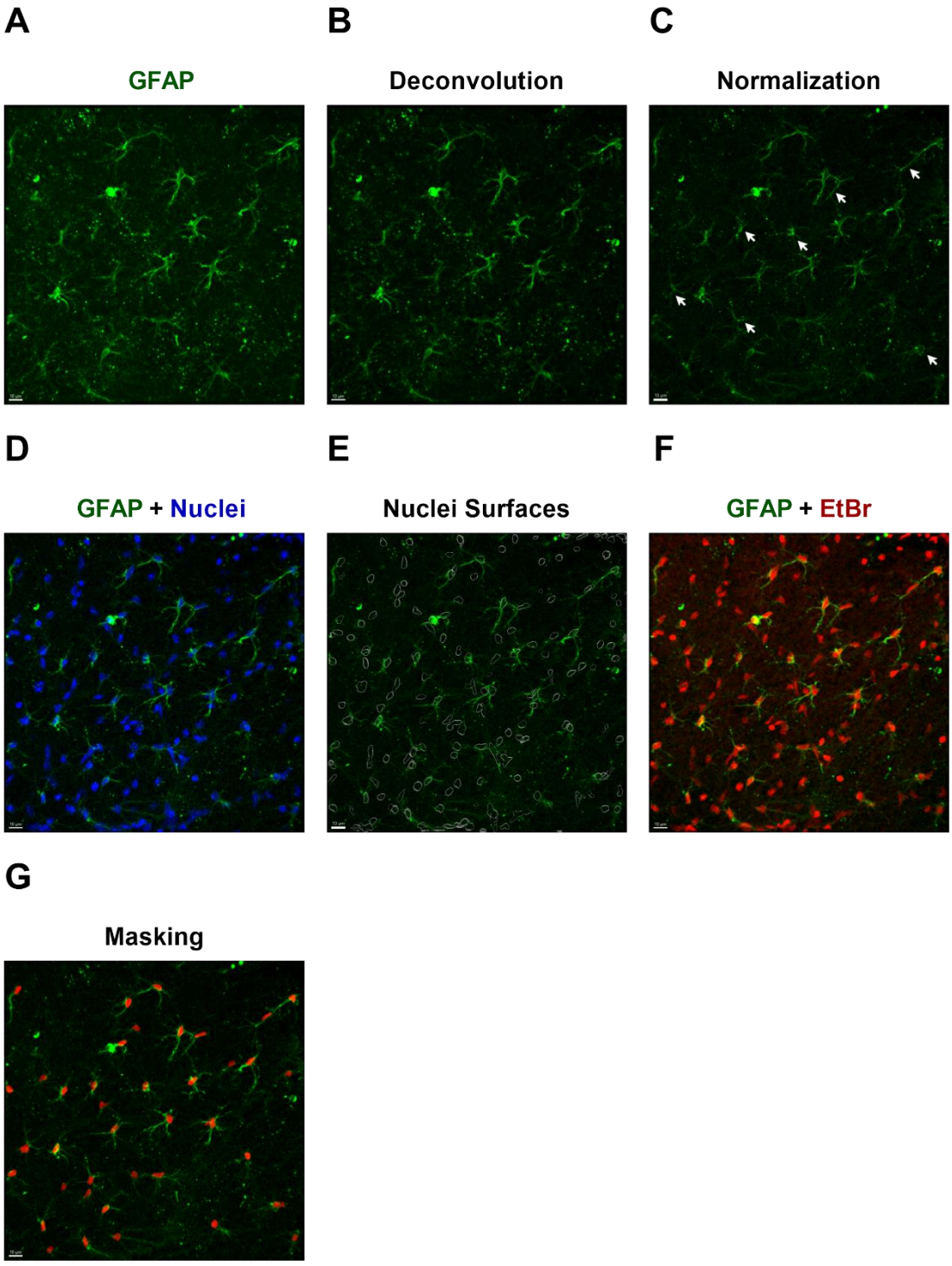

Figure 1 – Representative images of EtBr fluorescence signal (red) in a hippocampal section immunolabeled for GFAP (green) and further stained for nuclei (blue), depicting the image processing and analysis pipeline. Images of the pre-processing operations applied to the GFAP (488 nm) channel: (**A**) original, (**B**) deconvolved, and (**C**) deconvolved + normalized, where white arrows indicate unraveled GFAP$^+$ cells. (**D**) Overlay of GFAP and nuclei (405 nm) channels, and (**E**) segmentation of the nuclei channel by creating an Imaris *Surpass Object* of type *Surfaces*, which are represented in white. (**F**) Overlay of GFAP and EtBr (561 nm) channels, and (**G**) mask created from the EtBr channel after manual selection of the *Surfaces* corresponding to GFAP$^+$ cells. All scale bars: 10 µm.

2. $A_{2A}R$ blockade prevents $A\beta_{1-42}$-induced astrocytic HC activation

First, it was investigated whether *ex vivo* $A\beta_{1-42}$ exposure affects astrocytic HC activity in hippocampal slices from C57BL/6 mice. The results obtained demonstrated that hippocampal astrocytes from these mice treated with $A\beta_{1-42}$ (1 µM, 60 min) took up a significantly (p = 0.0475, paired t-test) greater amount of EtBr compared to non-treated hippocampal astrocytes ($A\beta_{1-42}$: 1.140 ± 0.103 au.µm^{-3} *vs* CTR: 0.5580 ± 0.0417 au.µm^{-3}, n = 4-5, Figure 2A). Then, it was evaluated whether $A_{2A}R$ regulate astrocytic HC activity by resorting to the selective $A_{2A}R$ antagonist SCH 58261. Two-way ANOVA followed by Sidak's multiple comparisons test showed that superfusion with SCH 58261 (50 nM, 90 min) *per se* did not alter EtBr uptake by astrocytes (SCH 58261: 0.497 ± 0.062 au.µm^{-3} *vs* CTR: 0.558 ± 0.042 au.µm^{-3}, n = 4). However, when SCH 58261 was applied 30 min prior to $A\beta_{1-42}$ challenge, the increase in EtBr uptake by astrocytes induced by $A\beta_{1-42}$ ($A\beta_{1-42}$: 1.135 ± 0.103 au.µm^{-3} *vs* CTR: 0.558 ± 0.042 au.µm^{-3}, n = 4-5, p = 0.0048) was significantly (p = 0.0031) reduced (SCH 58261 + $A\beta_{1-42}$: 0.690 ± 0.088 au.µm^{-3} *vs* $A\beta_{1-42}$: 1.135 ± 0.103 au.µm^{-3}, n = 5). Together, these data suggest that $A_{2A}R$ blockade prevents $A\beta_{1-42}$-induced increase in astrocytic HC activity (Figure 2B).

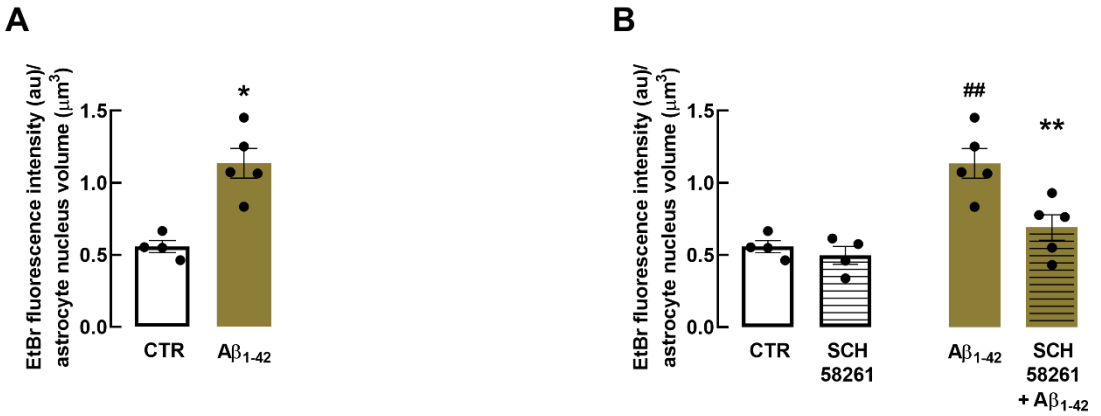

Figure 2 – *Ex vivo* $A\beta_{1-42}$ exposure increases HC activity in hippocampal astrocytes, which is prevented by $A_{2A}R$ pharmacological blockade. (**A**) EtBr fluorescence intensity (au) divided by astrocyte nucleus volume (µm^3) in hippocampal slices from C57BL/6 mice superfused with saline (CTR) or $A\beta_{1-42}$ (1 µM, 60 min). Data are mean ± SEM of n = 4-5 independent experiments, *p < 0.05, t-test (paired). (**B**) EtBr fluorescence intensity divided by astrocyte nucleus volume in hippocampal slices from C57BL/6 mice superfused with the selective $A_{2A}R$ antagonist SCH 58261 (50 nM, 90 min) and further challenged with $A\beta_{1-42}$ (SCH 58261 30 min prior to $A\beta_{1-42}$), being also shown the conditions of CTR and $A\beta_{1-42}$. Data are mean ± SEM of n = 4-5 independent experiments, **p < 0.01 *vs* $A\beta_{1-42}$, ##p < 0.01 *vs* CTR, two-way ANOVA (repeated measures) followed by Sidak's multiple comparisons test.

3. Astrocytic HC are activated in AD mouse models

In addition to $A\beta_{1-42}$-treated hippocampal slices, astrocytic HC activity was also examined in hippocampal slices from two AD mouse models, in specific mice injected icv with $A\beta_{1-42}$ recapitulating sporadic AD (Canas et al., 2009; Lopes et al., 2022), and APP/PS1 transgenic mice modeling familial AD (Izco et al., 2014). It was observed that hippocampal astrocytes from mice injected icv with $A\beta_{1-42}$ (2 nmol) displayed a significant (p = 0.0323, unpaired t-test) increase in EtBr uptake compared to mice injected icv with vehicle (icv-$A\beta_{1-42}$: 0.7940 ± 0.0711 au.µm^{-3} *vs* icv-VEH: 0.5580 ± 0.0417 au.µm^{-3}, n = 4-5, Figure 3A). Likewise, hippocampal astrocytes from APP/PS1 mice took up a significantly (p < 0.0001, unpaired t-test) greater amount of EtBr compared to WT littermates (APP/PS1: 0.5360 ± 0.0277 au.µm^{-3} *vs* WT: 0.3180 ± 0.0114 au.µm^{-3}, n = 5, Figure 3B).

The contribution of Cx43 HC to the overall astrocytic HC activity was analyzed by resorting to the Cx43 mimetic peptide Gap19, which specifically inhibits Cx43 HC without interfering with GJ communication (Abudara et al., 2014). Two-way ANOVA followed by Sidak's multiple comparisons test revealed that Gap19 did not alter EtBr uptake by astrocytes in hippocampal slices from WT mice (Gap19: 0.363 ± 0.031 au.µm^{-3} *vs* CTR: 0.318 ± 0.011 au.µm^{-3}, n = 5), which denotes that astrocytic Cx43 HC are predominantly inactive in basal conditions. In contrast, the increased EtBr uptake by astrocytes in hippocampal slices from APP/PS1 mice (APP/PS1: 0.536 ± 0.028 au.µm^{-3} *vs* WT: 0.318 ± 0.011 au.µm^{-3}, n = 5, p = 0.0006) was strongly (p = 0.0004) reduced by Gap19 (Gap19: 0.340 ± 0.052 au.µm^{-3} *vs* CTR: 0.536 ± 0.028 au.µm^{-3}, n = 5), indicating that astrocytic Cx43 HC are overactivated in APP/PS1 mice. Since the amount of EtBr took up by Gap19-treated APP/PS1 astrocytes (0.340 ± 0.052 au.µm^{-3}) was similar to that of non-treated WT astrocytes (0.318 ± 0.011 au.µm^{-3}), it can be concluded that most EtBr uptake occurred through astrocytic Cx43 HC, which is consistent with previous studies (*e.g.*, Orellana et al., 2011; Yi et al., 2016). This observation also allowed to exclude the hypothesis of unspecific EtBr uptake, for instance due to membrane injury (Figure 3C).

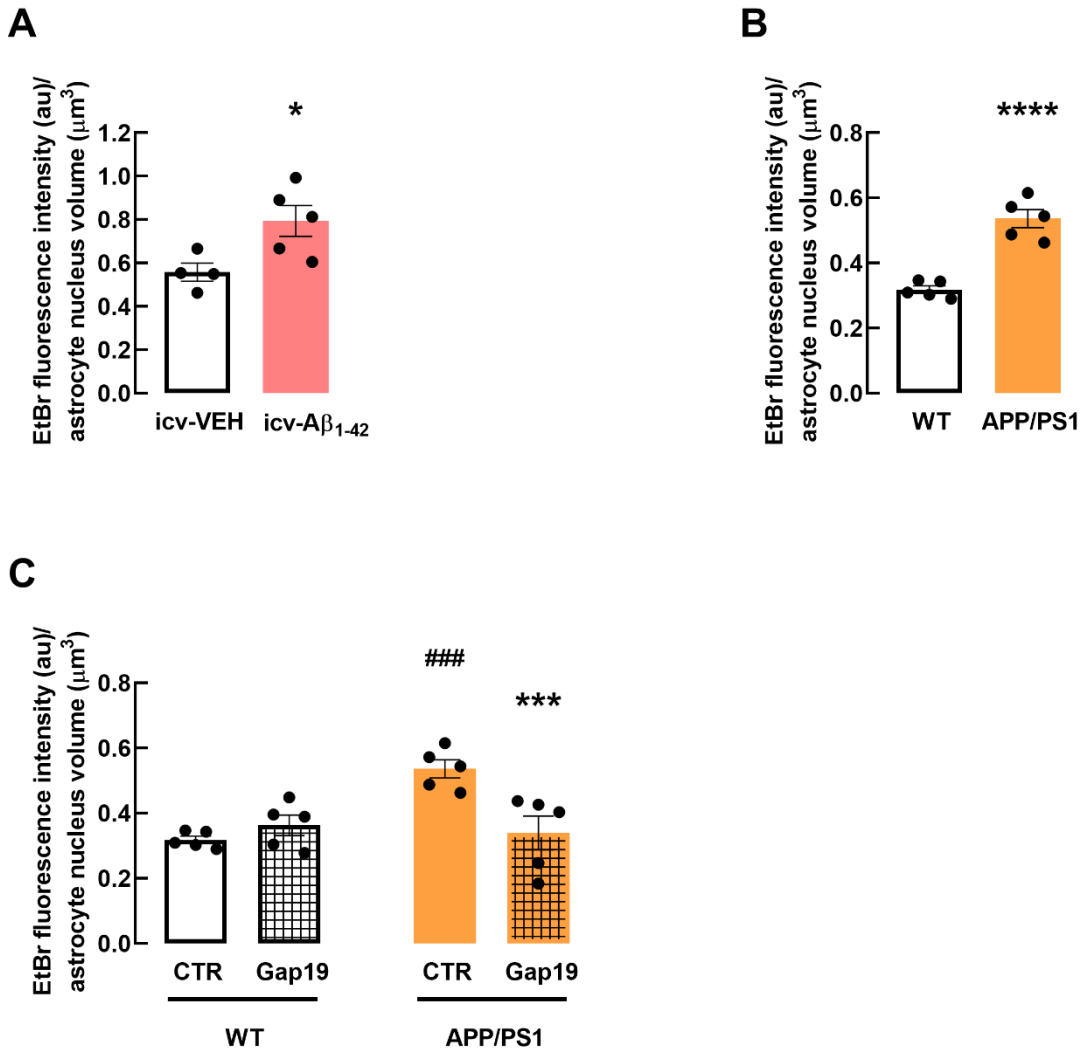

Figure 3 – HC activity is increased in hippocampal astrocytes from icv-Aβ$_{1-42}$ and APP/PS1 mice, and Cx43 HC pharmacological blockade decreases astrocytic HC activity of APP/PS1 mice to the level of WT mice. (**A**) EtBr fluorescence intensity (au) divided by astrocyte nucleus volume (µm^3) in hippocampal slices from mice injected icv with Aβ$_{1-42}$ (2 nmol) or vehicle, and (**B**) in hippocampal slices from APP/PS1 mice and WT littermates. Data are mean ± SEM of n = 4-5 independent experiments, *p < 0.05, ****p < 0.0001, t-test (unpaired). (**C**) EtBr fluorescence intensity divided by astrocyte nucleus volume in hippocampal slices from APP/PS1 mice and WT littermates, which were superfused with saline (CTR) or the Cx43 HC inhibitor Gap19 (250 µM, 90 min). Data are mean ± SEM of n = 5 independent experiments, ***p < 0.001 *vs* CTR, ###p < 0.001 *vs* WT, two-way ANOVA (repeated measures) followed by Sidak's multiple comparisons test.

4. Blockade of either $A_{2A}R$ or CD73-mediated adenosine formation does not reverse astrocytic HC activation in AD mouse models

Besides the purported prophylactic effect of $A_{2A}R$ blockade, as assessed in hippocampal slices superfused with the selective $A_{2A}R$ antagonist SCH 58261 prior to $A\beta_{1-42}$ challenge (see Figure 2B), it was further investigated whether $A_{2A}R$ blockade also translates into a presumed therapeutic effect. Two-way ANOVA followed by Sidak's multiple comparisons test showed that, in hippocampal slices from mice injected icv with vehicle, SCH 58261 (50 nM, 90 min) did not alter astrocytic EtBr uptake (SCH 58261: 0.497 ± 0.062 au.µm^{-3} *vs* CTR: 0.558 ± 0.042 au.µm^{-3}, n = 4). Furthermore, the increased astrocytic EtBr uptake in hippocampal slices from mice injected icv with $A\beta_{1-42}$ (icv-$A\beta_{1-42}$: 0.794 ± 0.071 au.µm^{-3} *vs* icv-VEH: 0.558 ± 0.042 au.µm^{-3}, n = 4-5, p = 0.0436) was not reversed after superfusion with SCH 58261 (SCH 58261: 0.855 ± 0.076 au.µm^{-3} *vs* CTR: 0.794 ± 0.071 au.µm^{-3}, n = 4-5, Figure 4A).

Next, the effect of the selective $A_{2A}R$ antagonist SCH 58261 was investigated in APP/PS1 transgenic mice. Furthermore, since CD73-derived adenosine is responsible for $A_{2A}R$ activation in mouse striatum (Augusto et al., 2013) and hippocampus (Gonçalves et al., 2019), the effect of the CD73 inhibitor AOPCP (100 µM, 90 min) was also tested. Two-way ANOVA followed by Tukey's multiple comparisons test showed that astrocytic EtBr uptake was not altered in hippocampal slices from WT mice superfused with either SCH 58261 (SCH 58261: 0.363 ± 0.039 au.µm^{-3} *vs* CTR: 0.318 ± 0.011 au.µm^{-3}, n = 5) or AOPCP (AOPCP: 0.310 ± 0.023 au.µm^{-3} *vs* CTR: 0.318 ± 0.011 au.µm^{-3}, n = 5). Moreover, neither SCH 58261 (SCH 58261: 0.528 ± 0.068 au.µm^{-3} *vs* CTR: 0.536 ± 0.028 au.µm^{-3}, n = 5) nor AOPCP (AOPCP: 0.580 ± 0.124 au.µm^{-3} *vs* CTR: 0.536 ± 0.028 au.µm^{-3}, n = 5) reversed the increased astrocytic EtBr uptake in hippocampal slices from APP/PS1 mice (APP/PS1: 0.536 ± 0.028 au.µm^{-3} *vs* WT: 0.318 ± 0.011 au.µm^{-3}, n = 5, p = 0.0018, Figure 4B). Taken together, the results obtained demonstrate that neither selective $A_{2A}R$ antagonism nor CD73 inhibition are able to reverse the increased astrocytic HC activity in AD mouse models, in specific icv-$A\beta_{1-42}$ and APP/PS1 mice, suggesting a lack of therapeutic effect of $A_{2A}R$ blockade.

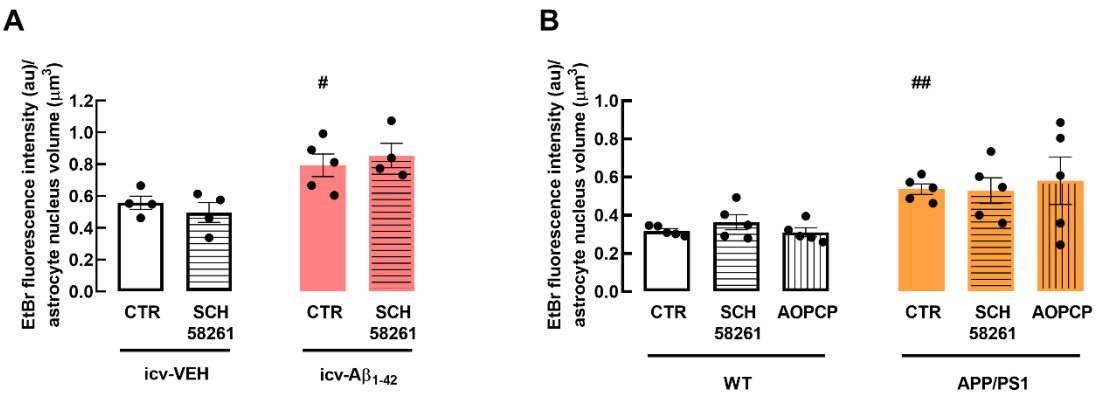

Figure 4 – Neither $A_{2A}R$ nor CD73 pharmacological blockade is able to reverse the increased HC activity in hippocampal astrocytes from icv-$A\beta_{1-42}$ and APP/PS1 mice. (**A**) EtBr fluorescence intensity (au) divided by astrocyte nucleus volume (μm^3) in hippocampal slices from mice injected icv with $A\beta_{1-42}$ (2 nmol) or vehicle, which were superfused with saline (CTR) or the selective $A_{2A}R$ antagonist SCH 58261 (50 nM, 90 min). (**B**) EtBr fluorescence intensity divided by astrocyte nucleus volume in hippocampal slices from APP/PS1 mice and WT littermates, which were superfused with either saline, SCH 58261 or the CD73 inhibitor AOPCP (100 μM, 90 min). Data are mean ± SEM of n = 4-5 independent experiments, $\#p < 0.05$ *vs* icv-VEH, $\#\#p < 0.01$ *vs* WT, two-way ANOVA (repeated measures) followed by Sidak's multiple comparisons test.

5. Silencing of astrocytic but not neuronal $A_{2A}R$ prevents $A\beta_{1-42}$-induced astrocytic HC activation

The long-term control of astrocytic HC activity by $A_{2A}R$ was examined using mice with global $A_{2A}R$ gene deletion. Two-way ANOVA followed by Sidak's multiple comparisons test revealed that $A\beta_{1-42}$ (1 μM, 60 min) significantly (p = 0.0023) increased EtBr uptake in hippocampal astrocytes from WT ($A_{2A}R^{+/+}$) mice ($A\beta_{1-42}$: 0.950 ± 0.072 au.μm^{-3} *vs* CTR: 0.667 ± 0.059 au.μm^{-3}, n = 3), but not from Gb-$A_{2A}R$ KO ($A_{2A}R^{-/-}$) mice ($A\beta_{1-42}$: 0.876 ± 0.034 au.μm^{-3} *vs* CTR: 0.891 ± 0.058 au.μm^{-3}, n = 3), indicating that full $A_{2A}R$ silencing prevents $A\beta_{1-42}$-induced increase in astrocytic HC activity (Figure 5A), similarly to that observed for acute $A_{2A}R$ blockade with the selective $A_{2A}R$ antagonist SCH 58261 (see Figure 2B). However, in basal conditions (that is, without treatment with $A\beta_{1-42}$), hippocampal astrocytes from Gb-$A_{2A}R$ KO mice displayed a significant (p = 0.0493) increase in EtBr uptake compared to WT mice ($A_{2A}R^{-/-}$: 0.891 ± 0.058 au.μm^{-3} *vs* $A_{2A}R^{+/+}$: 0.667 ± 0.059 au.μm^{-3}, n = 3), suggesting that full $A_{2A}R$ silencing *per se* increases astrocytic HC activity (Figure 5A), which contrasts with the lack of effect of SCH 58261 *per se* (see Figure 2B).

To assess the cellular origin (neurons, astrocytes or both) of $A_{2A}R$ that are supposed to regulate astrocytic HC activity, the extent of EtBr uptake by astrocytes was evaluated in hippocampal slices from mice with neuron- or astrocyte-specific $A_{2A}R$ gene deletion. Two-way ANOVA followed by Sidak's multiple comparisons test demonstrated that $A\beta_{1-42}$-treated hippocampal astrocytes from control ($A_{2A}R^{fl/fl\ +/+}$) mice took up a significantly (p = 0.0177 neuronal deletion, p = 0.0054 astrocytic deletion) greater amount of EtBr compared to non-treated hippocampal astrocytes ($A\beta_{1-42}$: 0.566 ± 0.024 au.µm^{-3} *vs* CTR: 0.410 ± 0.013 au.µm^{-3}, n = 4). In basal conditions, EtBr uptake by astrocytes was significantly increased in hippocampal slices from mice with neuron-specific $A_{2A}R$ gene deletion ($A_{2A}R^{fl/fl\ -/-}$: 0.569 ± 0.049 au.µm^{-3} *vs* $A_{2A}R^{fl/fl\ +/+}$: 0.410 ± 0.013 au.µm^{-3}, n = 4, p = 0.0443), as well as from mice with astrocyte-specific $A_{2A}R$ gene deletion (GFAP-$A_{2A}R^{fl/fl\ -/-}$: 0.512 ± 0.018 au.µm^{-3} *vs* $A_{2A}R^{fl/fl\ +/+}$: 0.410 ± 0.013 au.µm^{-3}, n = 4, p = 0.0200), compared to control mice. These findings suggest that cell-specific $A_{2A}R$ silencing enhances basal astrocytic HC activity (Figures 5B and 5D), as observed under full $A_{2A}R$ silencing (Figure 5A). Additionally, it was observed that $A\beta_{1-42}$ significantly (p = 0.0234) increased EtBr uptake in hippocampal astrocytes from mice with neuron-specific $A_{2A}R$ gene deletion ($A\beta_{1-42}$: 0.715 ± 0.064 au.µm^{-3} *vs* CTR: 0.569 ± 0.049 au.µm^{-3}, n = 4), indicating that neuron-specific $A_{2A}R$ silencing does not prevent the increase in astrocytic HC activity caused by $A\beta_{1-42}$ (Figure 5B). Interestingly, $A\beta_{1-42}$ did not alter EtBr uptake in hippocampal astrocytes from mice with astrocyte-specific $A_{2A}R$ gene deletion ($A\beta_{1-42}$: 0.523 ± 0.035 au.µm^{-3} *vs* CTR: 0.512 ± 0.018 au.µm^{-3}, n = 4), showing that although astrocyte-specific $A_{2A}R$ silencing *per se* slightly increases astrocytic HC activity, it is sufficient to prevent $A\beta_{1-42}$-induced increase in astrocytic HC activity (Figure 5D), similarly to that observed under full $A_{2A}R$ silencing (Figure 5A). Overall, these data demonstrate that astrocytic $A_{2A}R$ have a major role in the regulation of astrocytic HC activity upon $A\beta_{1-42}$ challenge.

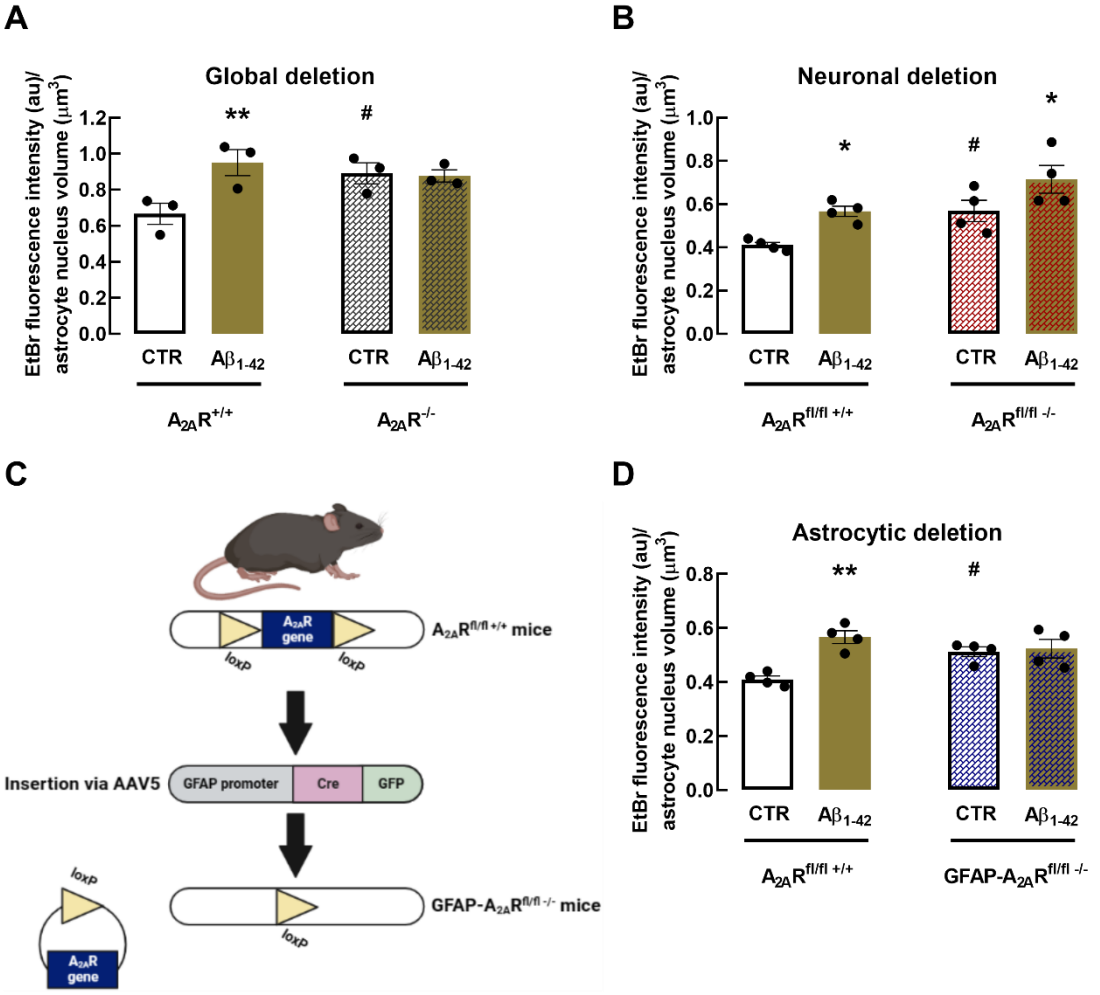

Figure 5 – Global $A_{2A}R$ gene deletion prevents $A\beta_{1-42}$-induced increase in HC activity in hippocampal astrocytes, an effect also observed when $A_{2A}R$ gene is specifically deleted from astrocytes but not from neurons. (**A**) EtBr fluorescence intensity (au) divided by astrocyte nucleus volume (μm^3) in hippocampal slices from Gb-$A_{2A}R$ KO mice ($A_{2A}R^{-/-}$) and WT littermates ($A_{2A}R^{+/+}$), which were superfused with saline (CTR) or $A\beta_{1-42}$ (1 μM, 60 min). (**B**) EtBr fluorescence intensity divided by astrocyte nucleus volume in hippocampal slices from Fb-$A_{2A}R$ KO mice ($A_{2A}R^{fl/fl\ -/-}$) and WT littermates ($A_{2A}R^{fl/fl\ +/+}$), which were superfused with saline or $A\beta_{1-42}$. (**C**) Schematic representation of the Cre/loxP system used to specifically silence $A_{2A}R$ in astrocytes through intracerebral injection of a viral transgenic construct (created in *BioRender.com*). (**D**) EtBr fluorescence intensity divided by astrocyte nucleus volume in hippocampal slices from mice with $A_{2A}R$ gene deletion in astrocytes (GFAP-$A_{2A}R^{fl/fl\ -/-}$) and age-matched control mice ($A_{2A}R^{fl/fl\ +/+}$), which were superfused with saline or $A\beta_{1-42}$. Data are mean ± SEM of n = 3-4 independent experiments, $*p < 0.05$ *vs* CTR, $**p < 0.01$ *vs* CTR, $\#p < 0.05$ *vs* $A_{2A}R^{+/+}$, $\#p < 0.05$ *vs* $A_{2A}R^{fl/fl\ +/+}$, two-way ANOVA (repeated measures) followed by Sidak's multiple comparisons test.

CHAPTER V

Discussion

Accumulating evidences suggest that astrocytic Cx43 is upregulated in AD patients (Nagy et al., 1996) and AD mouse models (Mei et al., 2010), and astrocytic HC composed of Cx43 are overactivated in primary astrocyte cultures and hippocampal slices exposed to synthetic $A\beta_{25-35}$ peptides (Orellana et al., 2011), as well as in hippocampal slices from AD transgenic mice (Yi et al., 2016), causing neuronal damage through excessive gliotransmitter release (Orellana et al., 2011; Yi et al., 2016). On the other hand, caffeine consumption inversely correlates with the incidence of AD (Maia and de Mendonça, 2002), and its apparent protective effects might be due to caffeine-mediated $A_{2A}R$ blockade (Dall'Igna et al., 2003; Dall'Igna et al., 2007). Indeed, $A_{2A}R$ density and activity are increased in the brain of AD patients (Albasanz et al., 2008). Astrocytic $A_{2A}R$ are also upregulated in AD patients and aged mice expressing human amyloid precursor protein, and the conditional knockout of astrocytic $A_{2A}R$ ameliorates memory in these mice (Orr et al., 2015). Recently, our group showed that, in cultured astrocytes challenged with synthetic $A\beta_{1-42}$ peptides, $A_{2A}R$ and Cx43 are physically associated, with the former triggering phosphorylation of the latter, which increases Cx43 HC activity, leading to increased ATP release. CD73 metabolizes ATP into adenosine, which is directed to $A_{2A}R$ activation, feeding a vicious circle (Madeira et al., 2021).

The present study investigated the putative $A_{2A}R$-mediated regulation of astrocytic Cx43 HC activity in hippocampal slices, which represent a more integrated biological system, where neuronal, glial and vascular interactions are present, under AD-like conditions. Furthermore, this work was also important to establish a three-dimensional image processing and analysis protocol for EtBr uptake experiments, which allow to assess HC activity. Indeed, analyzing the multi-slice stack (3D image), instead of overlapping the slices in a 2D image, avoids object overlay and subsequent "summation" of their fluorescence intensities, thus providing more accurate information about HC activity. For each hippocampal astrocyte (GFAP immuno-positive), EtBr fluorescence intensity

measured in the nucleus was divided by the volume of the nucleus, since larger nuclei can accumulate more EtBr resulting in higher EtBr fluorescence intensities.

Our data revealed that selective $A_{2A}R$ antagonism (with SCH 58261) prevents $A\beta_{1-42}$-induced increase in astrocytic HC activity. In contrast, it was observed that neither selective $A_{2A}R$ antagonism nor CD73 inhibition (with AOPCP) are able to reverse the increased astrocytic HC activity in AD mouse models, in specific in mice injected icv with $A\beta_{1-42}$ and APP/PS1 transgenic mice. Noteworthy, SCH 58261 and AOPCP were acutely applied, which might not be sufficient to counteract astrocytic HC overactivation that occurs in icv-$A\beta_{1-42}$-injected mice and APP/PS1 mice. Nevertheless, these pharmacological tools directed to $A_{2A}R$ might prove to be beneficial when long-term applied. This idea is supported by previous studies which report that the suppression of $A_{2A}R$ function has both a prophylactic (Canas et al., 2009; Gonçalves et al., 2019) and a therapeutic (Viana da Silva et al., 2016; Silva et al., 2018; Gonçalves et al., 2019) effect on synaptic plasticity and memory deficits under AD-like conditions.

Our results further demonstrated that full, neuron- or astrocyte-specific $A_{2A}R$ silencing enhances basal astrocytic HC activity, as opposed to selective $A_{2A}R$ antagonism, which has no effect *per se*. A likely explanation is that, although most HC are closed in basal conditions, some can open and have physiological roles, as supported by the observation that astrocytic Cx43 HC by releasing ATP are able to regulate basal excitatory synaptic transmission (Chever et al., 2014). In this regard, it is possible to speculate that the silencing of $A_{2A}R$, which are activated by ATP-derived adenosine (Gonçalves et al., 2019) and enhance NMDAR activity (Mouro et al., 2018), disrupts astrocytic Cx43 HC-mediated regulation of excitatory synaptic transmission, leading to aberrant astrocytic Cx43 HC activity, in basal conditions. On the other hand, upon $A\beta_{1-42}$ challenge, it was shown that astrocyte-specific $A_{2A}R$ silencing prevents a further increase in astrocytic HC activity, similarly to that observed under full $A_{2A}R$ silencing or selective $A_{2A}R$ antagonism. Interestingly, it was observed that neuron-specific $A_{2A}R$ silencing does not prevent $A\beta_{1-42}$-induced increase in astrocytic HC activity, which is particularly relevant since it allows to strengthen our hypothesis that astrocytic $A_{2A}R$ have a major role in the regulation of astrocytic HC activity in hippocampal slices exposed to synthetic $A\beta_{1-42}$ peptides.

Functioning as an important control of this work, the Cx43 HC inhibitor Gap19 reduced astrocytic EtBr uptake of APP/PS1 mice to the level of WT mice, allowing to exclude the hypothesis of unspecific uptake due to membrane injury, and revealing that

astrocytic Cx43 HC are preferentially activated in APP/PS1 mice. Indeed, if other connexin or pannexin channels were implicated, the reduction would be only partial. This is consistent with previous studies which report that Cx43 HC are the major contributors to the overall astrocytic HC activity, whereas Panx1 HC have a minor or insignificant contribution, under AD-like conditions (Orellana et al., 2011; Yi et al., 2016). Taken together, the results obtained demonstrated that the blockade of astrocytic $A_{2A}R$ prevents astrocytic Cx43 HC overactivation under AD-like conditions. It is worth noting that most HC inhibitors (with the exception of synthetic peptides as Gap19 that mimic cytoplasmic loop sequences) hamper HC docking, affecting GJ communication and, hence, many homeostatic functions ensured by astroglial networks (Abudara et al., 2014). In this context, $A_{2A}R$ antagonism might represent an alternative to Cx43 HC inhibition, in order to counteract astrocytic Cx43 HC overactivation, without compromising astrocytic GJ communication, under AD-like conditions.

Increased astrocytic Cx43 HC activity is reported to cause neuronal damage in primary astrocyte cultures and hippocampal slices exposed to synthetic $A\beta_{25-35}$ peptides (Orellana et al., 2011), as well as in hippocampal slices from AD transgenic mice (Yi et al., 2016). This allows to speculate that astrocytic Cx43 HC-mediated gliotransmitter release might sustain overactivation of purinergic and glutamatergic receptors under AD-like conditions. Although the present study focused on $A_{2A}R$, which are activated by ATP-derived adenosine, ATP can act directly on P_2R. In an AD mouse model, it was shown that astrocyte hyperactivity, consisting of Ca^{2+} transients in individual astrocytes and Ca^{2+} waves along astroglial networks, is regulated by HC-mediated ATP release and P_2Y_1R signaling (Delekate et al., 2014), and long-term P_2Y_1R blockade reduces astrocyte hyperactivity, restores synaptic function and reverses memory deficits (Reichenbach et al., 2018). Additionally, AD transgenic mice lacking P_2X_7R display reduced Aβ load and enhanced synaptic plasticity and memory (Martin et al., 2019). Moreover, HC may also release glutamate, whose extracellular levels are increased under AD-like conditions, overactivating extrasynaptic NMDAR that, ultimately, are internalized, impairing synaptic plasticity (reviewed in Guo et al., 2020).

CHAPTER VI

Conclusions and future directions

The present study strengthened the putative role of astrocytic $A_{2A}R$ in the regulation of astrocytic Cx43 HC activity, previously observed in primary astrocyte cultures and here in hippocampal slices (Figure 6). The data demonstrated that the blockade of astrocytic $A_{2A}R$ prevents astrocytic Cx43 HC overactivation under AD-like conditions, possibly with concomitant alleviation of gliotransmitter release.

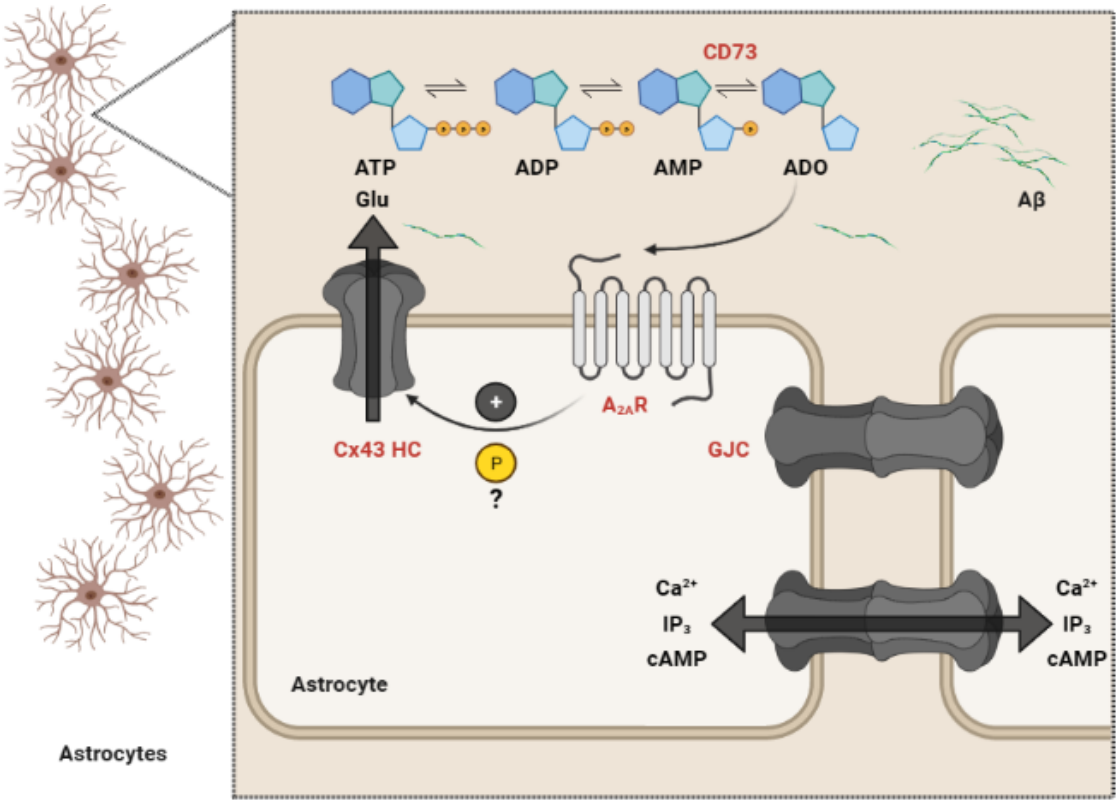

Figure 6 – Schematic representation of astrocytic $A_{2A}R$-mediated regulation of astrocytic Cx43 HC activity under conditions of Aβ exposure. Astrocytes are coupled through gap junction channels (GJC), allowing the diffusion of small signaling molecules, such as Ca^{2+}, inositol triphosphate (IP_3) and cyclic AMP (cAMP), between cells. The major GJC-forming protein, connexin 43 (Cx43), can also form unitary channels called hemichannels (HC), mediating the release of gliotransmitters, namely glutamate (Glu) and ATP. Upon amyloid-β (Aβ) challenge, adenosine A_{2A} receptors ($A_{2A}R$) regulate Cx43 HC activity, possibly via Cx43 HC phosphorylation, leading to increased ATP release. Ecto-5′-nucleotidase (CD73) dephosphorylates AMP into adenosine (ADO), the last and rate-limiting step of the enzymatic breakdown of extracellular ATP. CD73-derived ADO is directed to $A_{2A}R$ activation, feeding a vicious circle (created in *BioRender.com*).

In regard to future directions, it would be interesting to determine the molecular mechanism underlying $A_{2A}R$-mediated regulation of Cx43 HC activity in astrocytes. HC activity is highly regulated by Cx phosphorylation, and the role of astrocytic Cx43 HC phosphorylation is well-established upon ischemic insults, which trigger astrocytic Cx43 HC dephosphorylation, as first described in Li et al., 1998. However, little is known about the role of astrocytic Cx43 HC phosphorylation under AD-like conditions. Accordingly, our group previously showed that $A\beta_{1-42}$ triggers Cx43 HC phosphorylation in cultured astrocytes, an effect prevented by $A_{2A}R$ blockade (Madeira et al., 2021). Nevertheless, this $A_{2A}R$-mediated Cx43 HC phosphorylation, which might prompt Cx43 HC activation upon $A\beta_{1-42}$ challenge, was observed in primary astrocyte cultures and still remains to be confirmed in more complex experimental models, namely in mouse brain structures such as the hippocampus, where besides astrocytes there are other brain cells that establish physical and functional interactions with each other. A possible experimental design would consist of preparing mouse hippocampal gliosomes (purified membranes from astrocytic processes) and quantifying phospho-Cx43 levels via Western blot analysis. These experiments are already running in our lab through the expertise of Daniela Madeira.

REFERENCES

Abudara, V., Bechberger, J., Freitas-Andrade, M., De Bock, M., Wang, N., Bultynck, G., Naus, C. C., Leybaert, L., & Giaume, C. (2014). The connexin43 mimetic peptide Gap19 inhibits hemichannels without altering gap junctional communication in astrocytes. *Frontiers in Cellular Neuroscience*, 8, 306. https://doi.org/10.3389/fncel.2014.00306

Agostinho, P., Madeira, D., Dias, L., Simões, A. P., Cunha, R. A., & Canas, P. M. (2020). Purinergic signaling orchestrating neuron-glia communication. *Pharmacological Research*, 162, 105253. https://doi.org/10.1016/j.phrs.2020.105253

Albasanz, J. L., Perez, S., Barrachina, M., Ferrer, I., & Martín, M. (2008). Up-regulation of adenosine receptors in the frontal cortex in Alzheimer's disease. *Brain Pathology*, 18(2), 211–219. https://doi.org/10.1111/j.1750-3639.2007.00112.x

Andersson, M., Blomstrand, F., & Hanse, E. (2007). Astrocytes play a critical role in transient heterosynaptic depression in the rat hippocampal CA1 region. *The Journal of Physiology*, 585(3), 843–852. https://doi.org/10.1113/jphysiol.2007.142737

Angulo, E., Casadó, V., Mallol, J., Canela, E. I., Viñals, F., Ferrer, I., Lluis, C., & Franco, R. (2003). A_1 adenosine receptors accumulate in neurodegenerative structures in Alzheimer disease and mediate both amyloid precursor protein processing and tau phosphorylation and translocation. *Brain Pathology*, 13(4), 440–451. https://doi.org/10.1111/j.1750-3639.2003.tb00475.x

Araque, A., Parpura, V., Sanzgiri, R. P., & Haydon, P. G. (1999). Tripartite synapses: glia, the unacknowledged partner. *Trends in Neurosciences*, 22(5), 208–215. https://doi.org/10.1016/s0166-2236(98)01349-6

Arendash, G. W., Mori, T., Cao, C., Mamcarz, M., Runfeldt, M., Dickson, A., Rezai-Zadeh, K., Tane, J., Citron, B. A., Lin, X., Echeverria, V., & Potter, H. (2009). Caffeine reverses cognitive impairment and decreases brain amyloid-β levels in aged Alzheimer's disease mice. *Journal of Alzheimer's Disease*, 17(3), 661–680. https://doi.org/10.3233/JAD-2009-1087

Arendash, G. W., Schleif, W., Rezai-Zadeh, K., Jackson, E. K., Zacharia, L. C., Cracchiolo, J. R., Shippy, D., & Tan, J. (2006). Caffeine protects Alzheimer's mice against cognitive impairment and reduces brain β-amyloid production. *Neuroscience*, 142(4), 941–952. https://doi.org/10.1016/j.neuroscience.2006.07.021

Augusto, E., Matos, M., Sévigny, J., El-Tayeb, A., Bynoe, M. S., Müller, C. E., Cunha, R. A., & Chen, J. F. (2013). Ecto-5'-nucleotidase (CD73)-mediated formation of adenosine is critical for the striatal adenosine A_{2A} receptor functions. *The Journal of Neuroscience*, 33(28), 11390–11399. https://doi.org/10.1523/JNEUROSCI.5817-12.2013

Bastia, E., Xu, Y. H., Scibelli, A. C., Day, Y. J., Linden, J., Chen, J. F., & Schwarzschild, M. A. (2005). A crucial role for forebrain adenosine A_{2A} receptors in amphetamine sensitization. *Neuropsychopharmacology*, 30(5), 891–900. https://doi.org/10.1038/sj.npp.1300630

Bernardinelli, Y., Magistretti, P. J., & Chatton, J. Y. (2004). Astrocytes generate Na^+-mediated metabolic waves. *Proceedings of the National Academy of Sciences of the United States of America*, 101(41), 14937–14942. https://doi.org/10.1073/pnas.0405315101

Bitplane AG – An Oxford Instruments Company. *Imaris 9.6 Reference Manual*

Canas, P. M., Porciúncula, L. O., Cunha, G. M., Silva, C. G., Machado, N. J., Oliveira, J. M., Oliveira, C. R., & Cunha, R. A. (2009). Adenosine A_{2A} receptor blockade prevents synaptotoxicity and memory dysfunction caused by β-amyloid peptides via p38 mitogen-activated protein kinase pathway. *The Journal of Neuroscience*, 29(47), 14741–14751. https://doi.org/10.1523/JNEUROSCI.3728-09.2009

Chen, J. F., Huang, Z., Ma, J., Zhu, J., Moratalla, R., Standaert, D., Moskowitz, M. A., Fink, J. S., & Schwarzschild, M. A. (1999). A_{2A} adenosine receptor deficiency attenuates brain injury induced by transient focal ischemia in mice. *The Journal of Neuroscience*, 19(21), 9192–9200. https://doi.org/10.1523/JNEUROSCI.19-21-09192.1999

Chever, O., Lee, C. Y., & Rouach, N. (2014). Astroglial connexin43 hemichannels tune basal excitatory synaptic transmission. *The Journal of Neuroscience*, 34(34), 11228–11232. https://doi.org/10.1523/JNEUROSCI.0015-14.2014

Ciruela, F., Casadó, V., Rodrigues, R. J., Luján, R., Burgueño, J., Canals, M., Borycz, J., Rebola, N., Goldberg, S. R., Mallol, J., Cortés, A., Canela, E. I., López-Giménez, J. F., Milligan, G., Lluis, C., Cunha, R. A., Ferré, S., & Franco, R. (2006). Presynaptic control of striatal glutamatergic neurotransmission by adenosine A_1-A_{2A} receptor heteromers. *The Journal of Neuroscience*, 26(7), 2080–2087. https://doi.org/10.1523/JNEUROSCI.3574-05.2006

Cruz, N. F., Ball, K. K., & Dienel, G. A. (2010). Astrocytic gap junctional communication is reduced in amyloid-β-treated cultured astrocytes, but not in Alzheimer's disease transgenic mice. *ASN neuro*, 2(4), e00041. https://doi.org/10.1042/AN20100017

Cummings, J., Lee, G., Nahed, P., Kambar, M. E. Z. N., Zhong, K., Fonseca, J., & Taghva, K. (2022). Alzheimer's disease drug development pipeline: 2022. *Alzheimer's & dementia*, 8(1), e12295. https://doi.org/10.1002/trc2.12295

Cunha, G. M., Canas, P. M., Melo, C. S., Hockemeyer, J., Müller, C. E., Oliveira, C. R., & Cunha, R. A. (2008). Adenosine A_{2A} receptor blockade prevents memory dysfunction caused by β-amyloid peptides but not by scopolamine or MK-801. *Experimental Neurology*, 210(2), 776–781. https://doi.org/10.1016/j.expneurol.2007.11.013

Cunha, R. A. (2016). How does adenosine control neuronal dysfunction and neurodegeneration? *Journal of Neurochemistry*, 139(6), 1019–1055. https://doi.org/10.1111/jnc.13724

Dall'Igna, O. P., Fett, P., Gomes, M. W., Souza, D. O., Cunha, R. A., & Lara, D. R. (2007). Caffeine and adenosine A_{2a} receptor antagonists prevent β-amyloid (25-35)-induced cognitive deficits in mice. *Experimental Neurology*, 203(1), 241–245. https://doi.org/10.1016/j.expneurol.2006.08.008

Dall'Igna, O. P., Porciúncula, L. O., Souza, D. O., Cunha, R. A., & Lara, D. R. (2003). Neuroprotection by caffeine and adenosine A_{2A} receptor blockade of β-amyloid neurotoxicity. *British Journal of Pharmacology*, 138(7), 1207–1209. https://doi.org/10.1038/sj.bjp.0705185

Delekate, A., Füchtemeier, M., Schumacher, T., Ulbrich, C., Foddis, M., & Petzold, G. C. (2014). Metabotropic P2Y1 receptor signalling mediates astrocytic hyperactivity *in vivo* in an Alzheimer's disease mouse model. *Nature Communications*, 5, 5422. https://doi.org/10.1038/ncomms6422

Dias, L., Madeira, D., Dias, R., Tomé, Â. R., Cunha, R. A., & Agostinho, P. (2022). $A\beta_{1-42}$ peptides blunt the adenosine A_{2A} receptor-mediated control of the interplay between P_2X_7 and P_2Y_1 receptors mediated calcium responses in astrocytes. *Cellular and Molecular Life Sciences*, 79(8), 457. https://doi.org/10.1007/s00018-022-04492-y

Diehlmann, A., Ida, N., Weggen, S., Grünberg, J., Haass, C., Masters, C. L., Bayer, T. A., & Beyreuther, K. (1999). Analysis of presenilin 1 and presenilin 2 expression and processing by newly developed monoclonal antibodies. *Journal of Neuroscience Research*, 56(4), 405–419. https://doi.org/10.1002/(SICI)1097-4547(19990515)56:4<405::AID-JNR8>3.0.CO;2-F

Eskelinen, M. H., Ngandu, T., Tuomilehto, J., Soininen, H., & Kivipelto, M. (2009). Midlife coffee and tea drinking and the risk of late-life dementia: a population-based CAIDE study. *Journal of Alzheimer's Disease*, 16(1), 85–91. https://doi.org/10.3233/JAD-2009-0920

Fedele, D. E., Li, T., Lan, J. Q., Fredholm, B. B., & Boison, D. (2006). Adenosine A_1 receptors are crucial in keeping an epileptic focus localized. *Experimental Neurology*, 200(1), 184–190. https://doi.org/10.1016/j.expneurol.2006.02.133

Frost, G. R., & Li, Y. M. (2017). The role of astrocytes in amyloid production and Alzheimer's disease. *Open Biology*, 7(12), 170228. https://doi.org/10.1098/rsob.170228

Giaume, C., Koulakoff, A., Roux, L., Holcman, D., & Rouach, N. (2010). Astroglial networks: a step further in neuroglial and gliovascular interactions. *Nature Reviews Neuroscience*, 11(2), 87–99. https://doi.org/10.1038/nrn2757

Giaume, C., Orellana, J. A., Abudara, V., & Sáez, J. C. (2012). Connexin-based channels in astrocytes: how to study their properties. *Methods in Molecular Biology*, 814, 283–303. https://doi.org/10.1007/978-1-61779-452-0_19

Gonçalves, F. Q., Lopes, J. P., Silva, H. B., Lemos, C., Silva, A. C., Gonçalves, N., Tomé, Â. R., Ferreira, S. G., Canas, P. M., Rial, D., Agostinho, P., & Cunha, R. A. (2019). Synaptic and memory dysfunction in a β-amyloid model of early Alzheimer's disease depends on

increased formation of ATP-derived extracellular adenosine. *Neurobiology of Disease*, 132, 104570. https://doi.org/10.1016/j.nbd.2019.104570

Griffin, J. M., Fackelmeier, B., Fong, D. M., Mouravlev, A., Young, D., & O'Carroll, S. J. (2019). Astrocyte-selective AAV gene therapy through the endogenous GFAP promoter results in robust transduction in the rat spinal cord following injury. *Gene Therapy*, 26(5), 198–210. https://doi.org/10.1038/s41434-019-0075-6

Guo, T., Zhang, D., Zeng, Y., Huang, T. Y., Xu, H., & Zhao, Y. (2020). Molecular and cellular mechanisms underlying the pathogenesis of Alzheimer's disease. *Molecular Neurodegeneration*, 15(1), 40. https://doi.org/10.1186/s13024-020-00391-7

Haass, C., Hung, A. Y., & Selkoe, D. J. (1991). Processing of beta-amyloid precursor protein in microglia and astrocytes favors an internal localization over constitutive secretion. *The Journal of Neuroscience*, 11(12), 3783–3793. https://doi.org/10.1523/JNEUROSCI.11-12-03783.1991

Halassa, M. M., & Haydon, P. G. (2010). Integrated brain circuits: astrocytic networks modulate neuronal activity and behavior. *Annual Review of Physiology*, 72, 335–355. https://doi.org/10.1146/annurev-physiol-021909-135843

Hardy, J., & Selkoe, D. J. (2002). The amyloid hypothesis of Alzheimer's disease: progress and problems on the road to therapeutics. *Science*, 297(5580), 353–356. https://doi.org/10.1126/science.1072994

Hartlage-Rübsamen, M., Zeitschel, U., Apelt, J., Gärtner, U., Franke, H., Stahl, T., Günther, A., Schliebs, R., Penkowa, M., Bigl, V., & Rossner, S. (2003). Astrocytic expression of the Alzheimer's disease beta-secretase (BACE1) is stimulus-dependent. *Glia*, 41(2), 169–179. https://doi.org/10.1002/glia.10178

Huygens Remote Manager. (n.d.). *Huygens Remote Manager User Manual*. https://huygens-remote-manager.readthedocs.io/

Izco, M., Martínez, P., Corrales, A., Fandos, N., García, S., Insua, D., Montañes, M., Pérez-Grijalba, V., Rueda, N., Vidal, V., Martínez-Cué, C., Pesini, P., & Sarasa, M. (2014). Changes in the brain and plasma Aβ peptide levels with age and its relationship with cognitive impairment in the APPswe/PS1dE9 mouse model of Alzheimer's disease. *Neuroscience*, 263, 269–279. https://doi.org/10.1016/j.neuroscience.2014.01.003

Kajiwara, Y., Wang, E., Wang, M., Sin, W. C., Brennand, K. J., Schadt, E., Naus, C. C., Buxbaum, J., & Zhang, B. (2018). GJA1 (connexin43) is a key regulator of Alzheimer's disease pathogenesis. *Acta Neuropathologica Communications*, 6(1), 144. https://doi.org/10.1186/s40478-018-0642-x

Li, P., Rial, D., Canas, P. M., Yoo, J. H., Li, W., Zhou, X., Wang, Y., van Westen, G. J., Payen, M. P., Augusto, E., Gonçalves, N., Tomé, A. R., Li, Z., Wu, Z., Hou, X., Zhou, Y., IJzerman, A. P., Boyden, E. S., Cunha, R. A., Qu, J., … Chen, J. F. (2015). Optogenetic activation of intracellular adenosine A_{2A} receptor signaling in the hippocampus is sufficient

to trigger CREB phosphorylation and impair memory. *Molecular Psychiatry*, 20(11), 1339–1349. https://doi.org/10.1038/mp.2014.182

Li, W. E., Ochalski, P. A., Hertzberg, E. L., & Nagy, J. I. (1998). Immunorecognition, ultrastructure and phosphorylation status of astrocytic gap junctions and connexin43 in rat brain after cerebral focal ischaemia. *The European Journal of Neuroscience*, 10(7), 2444–2463. https://doi.org/10.1046/j.1460-9568.1998.00253.x

Lopes, C. R., Amaral, I. M., Pereira, M. F., Lopes, J. P., Madeira, D., Canas, P. M., Cunha, R. A., & Agostinho, P. (2022). Impact of blunting astrocyte activity on hippocampal synaptic plasticity in a mouse model of early Alzheimer's disease based on amyloid-β peptide exposure. *Journal of Neurochemistry*, 160(5), 556–567. https://doi.org/10.1111/jnc.15575

Lopes, C.*, Madeira, D.*, Domingues, J., Simões, A. P., Canas, P. M., Cunha, R. A., Agostinho, P. (2022, Abstract-poster presentation). The impact of silencing astrocytic A_{2A} receptors on hippocampal synaptic plasticity and memory. *VI Symposium of the Portuguese Glia Network*, October 18, Porto, Portugal. *co-first authors

Madeira, D., Dias, L., Santos, P., Cunha, R. A., Canas, P. M., & Agostinho, P. (2021). Association between adenosine A_{2A} receptors and connexin 43 regulates hemichannels activity and ATP release in astrocytes exposed to amyloid-β peptides. *Molecular Neurobiology*, 58(12), 6232–6248. https://doi.org/10.1007/s12035-021-02538-z

Maia, L., & de Mendonça, A. (2002). Does caffeine intake protect from Alzheimer's disease? *European Journal of Neurology*, 9(4), 377–382. https://doi.org/10.1046/j.1468-1331.2002.00421.x

Martin, E., Amar, M., Dalle, C., Youssef, I., Boucher, C., Le Duigou, C., Brückner, M., Prigent, A., Sazdovitch, V., Halle, A., Kanellopoulos, J. M., Fontaine, B., Delatour, B., & Delarasse, C. (2019). New role of P2X7 receptor in an Alzheimer's disease mouse model. *Molecular Psychiatry*, 24(1), 108–125. https://doi.org/10.1038/s41380-018-0108-3

Matos, M., Augusto, E., Machado, N. J., dos Santos-Rodrigues, A., Cunha, R. A., & Agostinho, P. (2012b). Astrocytic adenosine A_{2A} receptors control the amyloid-β peptide-induced decrease of glutamate uptake. *Journal of Alzheimer's Disease*, 31(3), 555–567. https://doi.org/10.3233/JAD-2012-120469

Matos, M., Augusto, E., Santos-Rodrigues, A. D., Schwarzschild, M. A., Chen, J. F., Cunha, R. A., & Agostinho, P. (2012a). Adenosine A_{2A} receptors modulate glutamate uptake in cultured astrocytes and gliosomes. *Glia*, 60(5), 702–716. https://doi.org/10.1002/glia.22290

Mei, X., Ezan, P., Giaume, C., & Koulakoff, A. (2010). Astroglial connexin immunoreactivity is specifically altered at β-amyloid plaques in β-amyloid precursor protein/presenilin1 mice. *Neuroscience*, 171(1), 92–105. https://doi.org/10.1016/j.neuroscience.2010.08.001

Merighi, S., Battistello, E., Casetta, I., Gragnaniello, D., Poloni, T. E., Medici, V., Cirrincione, A., Varani, K., Vincenzi, F., Borea, P. A., & Gessi, S. (2021). Upregulation of cortical A_{2A}

adenosine receptors is reflected in platelets of patients with Alzheimer's disease. *Journal of Alzheimer's Disease*, 80(3), 1105–1117. https://doi.org/10.3233/JAD-201437

Mookherjee, P., Green, P. S., Watson, G. S., Marques, M. A., Tanaka, K., Meeker, K. D., Meabon, J. S., Li, N., Zhu, P., Olson, V. G., & Cook, D. G. (2011). GLT-1 loss accelerates cognitive deficit onset in an Alzheimer's disease animal model. *Journal of Alzheimer's Disease*, 26(3), 447–455. https://doi.org/10.3233/JAD-2011-110503

Mouro, F. M., Rombo, D. M., Dias, R. B., Ribeiro, J. A., & Sebastião, A. M. (2018). Adenosine A_{2A} receptors facilitate synaptic NMDA currents in CA1 pyramidal neurons. *British Journal of Pharmacology*, 175(23), 4386–4397. https://doi.org/10.1111/bph.14497

Nagy, J. I., Li, W., Hertzberg, E. L., & Marotta, C. A. (1996). Elevated connexin43 immunoreactivity at sites of amyloid plaques in Alzheimer's disease. *Brain Research*, 717(1-2), 173–178. https://doi.org/10.1016/0006-8993(95)01526-4

Nedergaard, M., & Verkhratsky, A. (2012). Artifact versus reality-how astrocytes contribute to synaptic events. *Glia*, 60(7), 1013–1023. https://doi.org/10.1002/glia.22288

Oliveira, J. F., Sardinha, V. M., Guerra-Gomes, S., Araque, A., & Sousa, N. (2015). Do stars govern our actions? Astrocyte involvement in rodent behavior. *Trends in Neurosciences*, 38(9), 535–549. https://doi.org/10.1016/j.tins.2015.07.006

Orellana, J. A., Shoji, K. F., Abudara, V., Ezan, P., Amigou, E., Sáez, P. J., Jiang, J. X., Naus, C. C., Sáez, J. C., & Giaume, C. (2011). Amyloid β-induced death in neurons involves glial and neuronal hemichannels. *The Journal of Neuroscience*, 31(13), 4962–4977. https://doi.org/10.1523/JNEUROSCI.6417-10.2011

Orr, A. G., Hsiao, E. C., Wang, M. M., Ho, K., Kim, D. H., Wang, X., Guo, W., Kang, J., Yu, G. Q., Adame, A., Devidze, N., Dubal, D. B., Masliah, E., Conklin, B. R., & Mucke, L. (2015). Astrocytic adenosine receptor A_{2A} and G_s-coupled signaling regulate memory. *Nature Neuroscience*, 18(3), 423–434. https://doi.org/10.1038/nn.3930

Pagnussat, N., Almeida, A. S., Marques, D. M., Nunes, F., Chenet, G. C., Botton, P. H., Mioranzza, S., Loss, C. M., Cunha, R. A., & Porciúncula, L. O. (2015). Adenosine A_{2A} receptors are necessary and sufficient to trigger memory impairment in adult mice. *British Journal of Pharmacology*, 172(15), 3831–3845. https://doi.org/10.1111/bph.13180

Paiva, I., Carvalho, K., Santos, P., Cellai, L., Pavlou, M. A. S., Jain, G., Gnad, T., Pfeifer, A., Vieau, D., Fischer, A., Buée, L., Outeiro, T. F., & Blum, D. (2019). A_{2A}R-induced transcriptional deregulation in astrocytes: An in vitro study. *Glia*, 67(12), 2329–2342. https://doi.org/10.1002/glia.23688

Rebola, N., Lujan, R., Cunha, R. A., & Mulle, C. (2008). Adenosine A_{2A} receptors are essential for long-term potentiation of NMDA-EPSCs at hippocampal mossy fiber synapses. *Neuron*, 57(1), 121–134. https://doi.org/10.1016/j.neuron.2007.11.023

Reichenbach, N., Delekate, A., Breithausen, B., Keppler, K., Poll, S., Schulte, T., Peter, J., Plescher, M., Hansen, J. N., Blank, N., Keller, A., Fuhrmann, M., Henneberger, C., Halle,

A., & Petzold, G. C. (2018). P2Y1 receptor blockade normalizes network dysfunction and cognition in an Alzheimer's disease model. *The Journal of Experimental Medicine*, 215(6), 1649–1663. https://doi.org/10.1084/jem.20171487

Rouach, N., Koulakoff, A., Abudara, V., Willecke, K., & Giaume, C. (2008). Astroglial metabolic networks sustain hippocampal synaptic transmission. *Science*, 322(5907), 1551–1555. https://doi.org/10.1126/science.1164022

Scemes, E., & Giaume, C. (2006). Astrocyte calcium waves: what they are and what they do. *Glia*, 54(7), 716–725. https://doi.org/10.1002/glia.20374

Scientific Volume Imaging. (n.d.). *Huygens Deconvolution: Restore microscopy images*. https://svi.nl/Huygens-Deconvolution

Selkoe, D. J., & Hardy, J. (2016). The amyloid hypothesis of Alzheimer's disease at 25 years. *EMBO Molecular Medicine*, 8(6), 595–608. https://doi.org/10.15252/emmm.201606210

Silva, A. C., Lemos, C., Gonçalves, F. Q., Pliássova, A. V., Machado, N. J., Silva, H. B., Canas, P. M., Cunha, R. A., Lopes, J. P., & Agostinho, P. (2018). Blockade of adenosine A_{2A} receptors recovers early deficits of memory and plasticity in the triple transgenic mouse model of Alzheimer's disease. *Neurobiology of Disease*, 117, 72–81. https://doi.org/10.1016/j.nbd.2018.05.024

Sofroniew, M. V., & Vinters, H. V. (2010). Astrocytes: biology and pathology. *Acta Neuropathologica*, 119(1), 7–35. https://doi.org/10.1007/s00401-009-0619-8

Temido-Ferreira, M., Ferreira, D. G., Batalha, V. L., Marques-Morgado, I., Coelho, J. E., Pereira, P., Gomes, R., Pinto, A., Carvalho, S., Canas, P. M., Cuvelier, L., Buée-Scherrer, V., Faivre, E., Baqi, Y., Müller, C. E., Pimentel, J., Schiffmann, S. N., Buée, L., Bader, M., Outeiro, T. F., … Lopes, L. V. (2020). Age-related shift in LTD is dependent on neuronal adenosine A_{2A} receptors interplay with mGluR5 and NMDA receptors. *Molecular Psychiatry*, 25(8), 1876–1900. https://doi.org/10.1038/s41380-018-0110-9

The Jackson Laboratory. (n.d.). *B6.Cg-Tg(APPswe, PSEN1dE9)85Dbo/Mmjax*. https://www.jax.org/strain/005864

Ventura, R., & Harris, K. M. (1999). Three-dimensional relationships between hippocampal synapses and astrocytes. *The Journal of Neuroscience*, 19(16), 6897–6906. https://doi.org/10.1523/JNEUROSCI.19-16-06897.1999

Viana da Silva, S., Haberl, M. G., Zhang, P., Bethge, P., Lemos, C., Gonçalves, N., Gorlewicz, A., Malezieux, M., Gonçalves, F. Q., Grosjean, N., Blanchet, C., Frick, A., Nägerl, U. V., Cunha, R. A., & Mulle, C. (2016). Early synaptic deficits in the APP/PS1 mouse model of Alzheimer's disease involve neuronal adenosine A_{2A} receptors. *Nature Communications*, 7, 11915. https://doi.org/10.1038/ncomms11915

Yi, C., Mei, X., Ezan, P., Mato, S., Matias, I., Giaume, C., & Koulakoff, A. (2016). Astroglial connexin43 contributes to neuronal suffering in a mouse model of Alzheimer's disease. *Cell Death and Differentiation*, 23(10), 1691–1701. https://doi.org/10.1038/cdd.2016.63

Zhang, B., Gaiteri, C., Bodea, L. G., Wang, Z., McElwee, J., Podtelezhnikov, A. A., Zhang, C., Xie, T., Tran, L., Dobrin, R., Fluder, E., Clurman, B., Melquist, S., Narayanan, M., Suver, C., Shah, H., Mahajan, M., Gillis, T., Mysore, J., MacDonald, M. E., … Emilsson, V. (2013). Integrated systems approach identifies genetic nodes and networks in late-onset Alzheimer's disease. *Cell*, 153(3), 707–720. https://doi.org/10.1016/j.cell.2013.03.030